IN VITRO AND IN VIVO EFFICACY COMPARISON OF THREE CYANIDE ANTIDOTE CANDIDATES AND FLUORESCENT METHOD DEVELOPMENT FOR MEASURING THE SELECTED CYANIDE ANTIDOTE DIMETHYL TRISULFIDE AT LOW CONCENTRATIONS

_____

A Thesis

Presented to

The Faculty of the Department of Chemistry

Sam Houston State University

_____

In Partial Fulfillment

of the Requirements for the Degree of

Master of Science

_____

by

Ramesha Dilhani Gaspe Ralalage

May, 2018

IN VITRO AND IN VIVO EFFICACY COMPARISON OF THREE CYANIDE ANTIDOTE CANDIDATES AND FLUORESCENT METHOD DEVELOPMENT FOR MEASURING THE SELECTED CYANIDE ANTIDOTE DIMETHYL TRISULFIDE AT LOW CONCENTRATIONS

by

Ramesha Dilhani Gaspe Ralalage

_____

APPROVED:

Ilona Petrikovics, PhD
Thesis Director

Donovan C. Haines, PhD
Committee Member

David E. Thompson, PhD
Committee Member

John B. Pascarella, PhD
Dean, College of Humanities and Social Sciences

DEDICATION

I would like to dedicate my thesis to:

- My parents and my brother who have always loved me unconditionally
- My loving husband, Pathum Madushanka Weerasekara, who has been a constant source of support and encouragement
- My research supervisor, Dr. Ilona Petrikovics, for the guidance, encouragement and advice she has provided throughout my time
- All the teachers I met throughout my entire life that enriched my knowledge, character and beliefs

ABSTRACT

Gaspe Ralalage, Ramesha Dilhani, *In vitro and in vivo efficacy comparison of three cyanide antidote candidates and fluorescent method development for measuring the selected cyanide antidote Dimethyl trisulfide at low concentrations*. Master of Science (Chemistry), May, 2018, Sam Houston State University, Huntsville, Texas.

Cyanide (CN) is a toxic molecule that inhibits oxygen utilization by cells. Thiosulfate converts CN^- into the less toxic thiocyanate (SCN^-), a reaction that is catalyzed by rhodanese (Rh). The comparison of sulfur donor (SD) efficacy (*in vitro)* and antidotal efficacy (*in vivo)* of different SDs (SD_1, SD_2 and SD_3) is described in the first part. The *in vitro* SD efficacy was monitored by quantifying the formation of SCN^- with and without Rh at physiological pH (7.4) and the optimum pH for Rh (8.6). The *in vitro* SD efficacy without Rh at pH 7.4 and with Rh at both pH values varies in the order of $SD_1 > SD_2 > SD_3$. The *in vivo* antidotal efficacies were expressed and compared using the antidotal potency ratios (APR) (APR= CN LD_{50} with antidote/CN LD_{50} without antidote). Mice were injected with CN and SD_1 and the APR value was calculated. The antidotal efficacy varies in the order of $SD_2 > SD_1 > SD_3$. The *in vitro* SD efficacy values and *in vivo* antidotal efficacy values were different due to several pharmacokinetic reasons. In the second part, a fluorescent method to detect low concentrations of DMTS (below 1 μg/mL) in blood samples is described. DMTS is a sulfane sulfur type CN antidote. Sulfane sulfur probe (SSP4) is a probe that selectively binds with sulfane sulfurs. Upon the reaction of SSP4 and DMTS, a fluorescent product is expected. The mixture of SSP4 and DMTS was scanned to determine its excitation and emission characteristics using a fluorescence spectrophotometer. The fluorescent product yielded from the reaction between SSP4 and DMTS exhibited peak absorbance at 280 nm and peak emission at 309 nm. A calibration curve was obtained at $\lambda_{ex}/\lambda_{em}$=280/309 nm for fluorescence intensity *vs.* DMTS

concentrations (R^2=0.9935). The mixture of SSP4 and DMTS/ACN was then analyzed using an HPLC-fluorescence experiment with $\lambda_{ex}/\lambda_{em}$=280/309 nm. A fluorescent peak with a retention time of 11.1 minutes showed good linear correlation with DTMS concentration in simple aqueous solutions of DMTS (R^2=0.993), and in DMTS-spiked blood (R^2=0.9995).

KEY WORDS: Cyanide, Sulfane Sulfur, Sulfur Donor Efficacy, Dimethyl Trisulfide, Fluorescent Method Development, Sulfane Sulfur Probe.

ACKNOWLEDGEMENTS

I would like to express the deepest appreciation to my supervisor Dr. Ilona Petrikovics for the wisdom she bestowed upon me, unwavering support, prompt inspirations, guidance and encouragement to successfully complete this project. I am grateful to her for being a constant source of motivation and the skills and knowledge which I have gained through the project. I am highly indebted to my committee members Dr. Donovan C. Haines and Dr. David E. Thompson for taking part in useful decisions, giving necessary advice, unceasing encouragement, constructive criticism and support. I am very thankful to Dr. Richard E. Norman for his valuable suggestions and knowledge during my research.

I wish to express my sincere thanks to Dr. Afshin Ebrahimpour, previous postdoctoral researcher in Dr. Petrikovics's lab for his valuable guidance, supervision and tremendous help to initiate and proceeding this research. I would also like to acknowledge and thank Dr. Marton Kiss, current postdoctoral researcher in Dr. Petrikovics's lab for his insightful suggestions, extreme patience, endless support and understanding spirit during this project. A very special thanks to all the professors and staff in Department of Chemistry for facilitating a great environment for research and learning.

I would like to convey my gratefulness to all my dear friends in Dr. Petrikovics's lab and the Department of Chemistry for their encouragement and moral support which made my studies more enjoyable.

I have no valuable words to express my deepest gratitude to my dear parents and my loving brother for their unconditional trust and love, timely encouragement and endless patience.

I owe thanks to a very special person, my husband for his continued and unfailing love, support and understanding during my Master's degree that made the completion of thesis possible. You were always around at times I thought that it is impossible to continue, you helped me to keep things in perspective.

TABLE OF CONTENTS

Page

LIST OF TABLES

LIST OF FIGURES

Figure **Page**

CHAPTER I

INTRODUCTION

PART 1

Toxicity and Sources of Cyanide (CN)

In 1706, the paint maker Diesbach discovered the Prussian Blue pigment serendipitously[1] and later a chemist, Pierre Macquer, realized that Prussian Blue could be oxidized to yield a gas.[2] Gay-Lussac condensed this 'unknown acidic gas' into a light blue liquid and named it "cyanide" because the Greek word for blue is "cyan".[3] Abiotically produced CN is present in the cosmos and was first detected in the interstellar medium.[4] Volcanic eruptions and lightning-induced reactions also release CN abiotically to the environment. Biotically produced CN compounds are also present in the environment. Plants and some animal species produce CN containing compounds as a defense mechanism against herbivores and predators. Cyanogenic glycosides are bio-active molecules that liberate CN as a protective mechanism against herbivores and pathogens.[5] Low levels of cyanogenic glycosides are present in apricot seeds, bean sprouts, cashews, cherry seeds, chestnuts and corn. Almonds and cassava roots contain considerable amounts of cyanogenic glycosides. CN can also be released to the environment by burning certain polymers such as polyacrylonitrile, polyurethane, polyamide, wool, silk and rubber.[6]

CN has been reported as a terrorist threat due to its toxic effect, wide availability and low production cost.[7] It is used in gold mining, textile manufacturing and electroplating processes.[7] Since CN is a weak acid with pKa of 9.2, it is mainly present in the form of HCN at the body's pH of 7.4.[6] This nonionic form can easily cross the cellular and subcellular membranes in the body. CN binds metal ion containing enzymes in the body

with high affinity. The most important of these is the cytochrome c oxidase, the terminal oxidase in the mitochondrial electron transport chain.[6] Once CN binds with the ferric ion in the cytochrome c oxidase enzyme it inhibits the oxygen utilization by the cells.[8] This condition is called cellular hypoxia. As a result of the inhibition of the aerobic pathway, an anaerobic pathway becomes dominant which leads to lactic acidosis.[6] Lower CN doses are responsible for dizziness, headache, nausea and vomiting.[9] With high CN exposure, cardiogenic shock can be generated due to pulmonary arteriolar and coronary vasoconstriction.[9] Chemoreceptors in the carotid artery and the aorta can be stimulated by CN, followed by hyperapnea.[6] Furthermore, higher doses of CN can cause severe tissue damage and death. The LD_{50} values for potassium cyanide (KCN) in humans and mice are 3.26 mg/kg[10] and 10.9 mg/kg[7], respectively.

Prior to studying mechanisms for antagonizing CN in a murine model, it is useful to estimate the CN concentration that would be present in the circulation if a mouse was given an LD_{50} dose of CN. The subcutaneous LD_{50} value for KCN is 10.9 mg/kg for mice. On average, mice have around 725 mL/kg of total body water (blood + intra and extracellular water).[11] The concentration of CN in the total body water at the dose equal to LD_{50} (10.9 mg/kg) is (10.9 mg/kg / (725 mL/kg* 65.12 g/mol)) = 0.23 mM.

CN can be eliminated from the body by pulmonary exhalation, urinary excretion, and biotransformation.[12] The body has CN detoxification mechanisms for endogenous CN. The sulfuration of CN^- has been identified as the main *in vivo* CN detoxification mechanism in the human body.[13] Upon sulfuration, CN^- is converted to the less toxic metabolite thiocyanate (SCN^-) which can be eliminated easily from the body. Biotransformation of CN involves both enzymatic and non-enzymatic reactions, however,

the dominant conversion mechanisms are enzymatic. The enzymatic conversion of CN^- into SCN^- is catalyzed by two major sulfurtransferase enzymes; rhodanese (Rh) and 3-mercaptopyruvate sulfurtransferase. Sometimes, albumin can also function as a sulfurtransferase.[12]

Thiosulfate ($S_2O_3^{2-}$) is the major endogenous sulfur donor (SD) for the sulfurtransferase Rh.[12] The rate of conversion of CN^- into SCN^- by SDs *in vitro* is called the SD efficacy. However, the sulfuration of CN^- by endogenous SDs such as $S_2O_3^{2-}$ is limited due to the depletion of the sulfane sulfur pool in the body. Therefore, restoration of the sulfur pool by the addition of exogenous sulfane sulfur is an important therapeutic strategy for the detoxification of CN^-.[12]

The aim of the first part of this study was to compare the *in vitro* and *in vivo* efficacy of three SD-type CN antidote candidate molecules which were labeled as SD_1, SD_2 and SD_3. All three SDs were tested *in vitro* and the SD efficacies were evaluated. Only the efficacy of SD_1 was tested in the present experiment *in vivo*, because SD_2 and SD_3 had been previously tested *in vivo* in Dr. Petrikovics's lab. The *in vivo* SD_1 data obtained in this study was compared to the data obtained from the prior *in vivo* tests of SD_2 and SD_3. (As Dr. Petrikovics's lab is working with the United States Army Medical Research Institute of Chemical Defense (USAMRICD) collaboratively, and the names of the SDs can't be revealed based on the rules and regulations of the two parties).

For the *in vitro* study, the standard protocol of the spectrophotometric assay of Westley[14] was used. Based on the *in vitro* data, a suitable initial KCN dose was selected for the test molecule SD_1 in the *in vivo* efficacy study. For the control, a suitable dose of KCN was used as the initial dose according to the Dixon and Massey's Software.[15]

CN Antidotes

Scientists began investigating CN antagonism prior to the 1930s. CN antidotes have historically fallen into one of two categories based on whether they bind CN to form a less toxic complex (Scavengers), or chemically transform CN into a less toxic form (Chemical Transformers).

(a) Scavengers

Methemoglobin Formers

Because CN shows high binding affinity towards methemoglobin, and forms a relatively stable cyanomethemoglobin complex,[16] the methemoglobin former amyl nitrite was the first modern antidote for CN intoxication. Sodium nitrite is another methemoglobin former that has been extensively used as a CN antidote. Since, nitrites were identified as slow methemoglobin formers, 4-dimethylaminophenol (DMAP) was developed and investigated later as a faster methemoglobin former.[17]

Hydroxocobalamin

Cobalt compounds, such as hydroxocobalamin can be used as CN antidotes because they show high binding affinity to CN. Hydroxocobalamin is a metalloprotein, also known as a vitamin B12 precursor.[6] Hydroxocobalamin is the hydroxylated active form of cobalamin, which has a porphyrin like corrin ring that contains a single cobalt ion bound to the benzimidazolyl residue. Hydroxocobalamin binds CN and in this manner lowers CN levels in the blood stream. Once CN binds with hydroxocobalamin it forms cyanocobalamin which can easily be eliminated from the body.[6]

Cobinamide

Cobinamide is a cobalamin derivative that lacks the lower axial position dimethylbenzimidazole group coordinating the cobalt ion. Cobinamide has two ligand binding sites, the upper and lower while cobalamin has only the upper binding site.[6] Therefore cobinamide shows higher binding affinity towards CN than cobalamin. Furthermore, the dimethylbenzimidazole group has a negative trans-effect towards the incoming CN ligands which further reduces the affinity for CN in the case of cobalamin. In addition, cobinamide has five times higher water solubility than hydroxocobalamin.

(b) Chemical Transformers

Carbonyl Compounds

CN^- is a nucleophile that can attack carbonyl compounds such as aldehydes and ketones resulting in the formation of cyanohydrins. The advantages of carbonyl compounds over the classic CN antidote thiosulfate and nitrite are that the carbonyl compounds can penetrate more readily through the cellular and subcellular membranes.[6] Sodium pyruvate and alpha-ketoglutaric acid have been reported as potent CN antidotes.[18,19]

Sulfur Donors (SDs)

SD type antidotes react with CN to form the less toxic SCN anion (Figure 1).

$$CN^- + [Sulfane\ Sulfur] \overset{Rh}{\rightarrow} SCN^-$$

Figure 1. Conversion of CN^- into SCN^- Catalyzed by Rh. SCN^- is the less toxic urinary metabolite which can easily be eliminated from the body.

Sulfane sulfurs are molecules containing multiple divalent sulfur atoms bound to each other.[6] Sodium thiosulfate ($Na_2S_2O_3$) replaces endogenous thiosulfate and has been the most widely used sulfur donor antidote. Also, cystine, cysteine and glutathione are

examples for endogenous organo-sulfur molecules that have been investigated as CN antidotes.[20] They can act as SDs for the Rh enzyme in the biotransformation of CN^- into SCN^-. Many of the sulfur donor antidotes come from the sulfane sulfur family of compounds. This family of compounds includes:[21]

(a) Thiosulfates ($S_2O_3^{2-}$)

(b) Thiosulfonates (RSO_2S^-)

(c) Polythionates ($O_3S\text{-}S_X\text{-}SO_3^{2-}$)

(d) Persulfides ($R\text{-}S\text{-}S^-$)

(e) Elementary sulfur (staggered 8-membered ring)

(f) Polysulfides ($R\text{-}S\text{-}S_X\text{-}S\text{-}R$)

Some sulfanes (such as thiosulfate) are effective and safe CN antiodes. However, others have unfavorable pharmacokinetic parameters and/or toxicity that prevents them from being effectively used as SD antidotes for CN intoxication.[22]

Presently Available CN Antidotes and their Drawbacks

The two CN antidotal therapies that are currently available in the United States are Nithiodote™ and Cyanokit®. Nithiodote™ consists of $Na_2S_2O_3$ and $NaNO_2$. The Cyanokit® contains hydroxocobalamin as the active component. Both presently available antidotal therapies possess some drawbacks; they are not suitable for a mass casualty scenario and require intravenous administration by a trained person.[22] Moreover, Cyanokit® requires a high injection volume.[23] In the case of Nithiodote™, the effective conversion of CN^- into SCN^- requires high amount of thiosulfate. Additionally, the higher Rh dependency of thiosulfate and its poor membrane permeability to reach the mitochondrial Rh make Nithiodote™ a less effective CN antidote. Additionally, nitrite at higher dosage can cause

methemoglobinemia.[24] The disadvantages of the inorganic thiosulfate can be overcome by using SDs with greater lipophilicity. Intramuscular (IM) injection of antidotes are under examination in order to determine their potential effectiveness in case of mass scenarios. Therefore, various SDs are being studied and tested as CN antidotes.[25] Previous studies proved that certain organic thiosulfonates showed higher CN conversion efficacy than thiosulfate.[26]

Figure 2. Currently Available Therapeutic Agents Against CN Intoxication in USA. Both are administrated intravenously.

Origin of Dimethyl Trisulfide (DMTS)

Garlic and onion belong to the *Allium* genus and are rich in sulfur containing molecules. Early chemists have revealed that cutting garlic or onion bulbs releases a number of low molecular weight organo-sulfur compounds.[27] These molecules can be categorized into two types; allylcysteine (alliin) and γ-glutamylcysteines. Alliin and some of the γ-glutamylcysteines are converted into cysteine sulfoxides within the garlic bulbs. Upon cutting or chopping the garlic bulbs, alliinase enzyme is released which catalyzes the conversion of cysteine sulfoxides into allicin[27]. Allicin is responsible for the typical odor of garlic. It can break down to produce organo-sulfur compounds such as diallyl sulfide, diallyl disulfide, diallyl trisulfide. These compounds are further transformed to allylmethyl

sulfide, dimethyl disulfide and DMTS. Each gram of the garlic bulb contains 15-19 µg of DMTS. It is also found in many other natural sources such as aging beer, cabbage, broccoli and cauliflower. DMTS is being used as food flavoring and fragrance agent in the food industry.[28]

DMTS as a SD

Consequently, searching for more efficient organic SDs, DMTS was found to be a superior SD than thiosulfate with greater CN^- conversion efficacy, low Rh dependency and higher lipophilicity to reach the mitochondrial Rh.[29] DMTS, the simplest organic trisulfide, can be considered as a promising next generation scavenger-type CN antidote candidate. It is a pale yellow, oily, clear liquid with an unpleasant, foul odor. As a highly lipophilic molecule, it has a much higher solubility in organic solvents than in water (water solubility = 0.13 mg/mL).[25] As a potent SD type CN antidote, DMTS and its formulation with polysorbate 80 (Poly 80) for IM administration have been patented by Sam Houston State University (US 20150290143 A1, 2015; US 20150297535 A1, 2015).[30,31]

Thiosulfate: Cyanide Sulfur Transferase (EC 2.8.1.1), Rhodanese (Rh), and it's Tissue Distribution

The enzyme Rh is one of the sulfur transferase enzymes present in our body. It is a highly conserved and ubiquitous enzyme. Rh regulates the sulfur flux[32] in the cells and the synthesis of iron-sulfur centers in the electron transport chain. Sulfuration of CN^- is the best-known reaction catalyzed by the Rh.

$$CN^- + S_2O_3^{2-} \rightarrow SO_3^{2-} + SCN^-$$

Figure 3. Sulfuration of CN^- by $S_2O_3^{2-}$. This reaction is catalyzed by Rh.

It has been reported that the isolated crystalline Rh from mammalian sources is a small monomeric protein with a ~32 kDa molecular weight. It contains one reaction site per molecule.[33] The bovine mitochondrial Rh has a single polypeptide chain containing 293 amino acids. The polypeptide chain is folded into two domains which are equal in size.[34] The active site of the enzyme is a pocket located close to the interface of the two domains. The Cys-247 amino acid residue in the active site of the enzyme participates in the sulfur transfer reaction.[35]

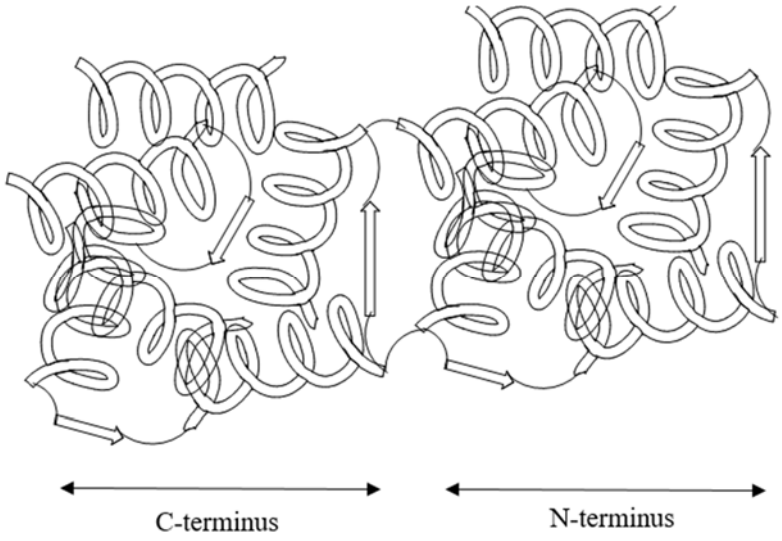

Figure 4. Three-Dimensional Structure of the Bovine Mitochondrial Rh. The single polypeptide chain is separated into two domains. The α-helices and β-sheets are shown as helices and arrows accordingly.[34]

Scientists have revealed that Rh is present in all living organisms, from bacteria to humans. It was found in many tissues of animals, such as liver, kidney and gastric mucosa.[36] Isoenzymes of Rh have been identified by electrophoretic methods followed by staining.[36] Rh is involved in CN detoxification in the body. In addition to that, it participates in the formation of iron sulfur centers,[37] energy metabolism[38] and acts as a thioredoxin oxidase.[39]

Role of Rh in the Conversion of CN^- into SCN^-

Rh catalyzes the CN^- conversion reaction through a double displacement mechanism where the sulfur atom from a suitable SD is transferred irreversibly to the nucleophilic center of CN^-. According to the kinetic studies, this mechanism involves two steps.[35] The sulfane sulfur atom of the SD is first transferred to the active site of Rh, forming a sulfur substituted enzyme. The sulfane sulfur is then transferred from the sulfur substituted enzyme to CN^-, yielding SCN^-.[35]

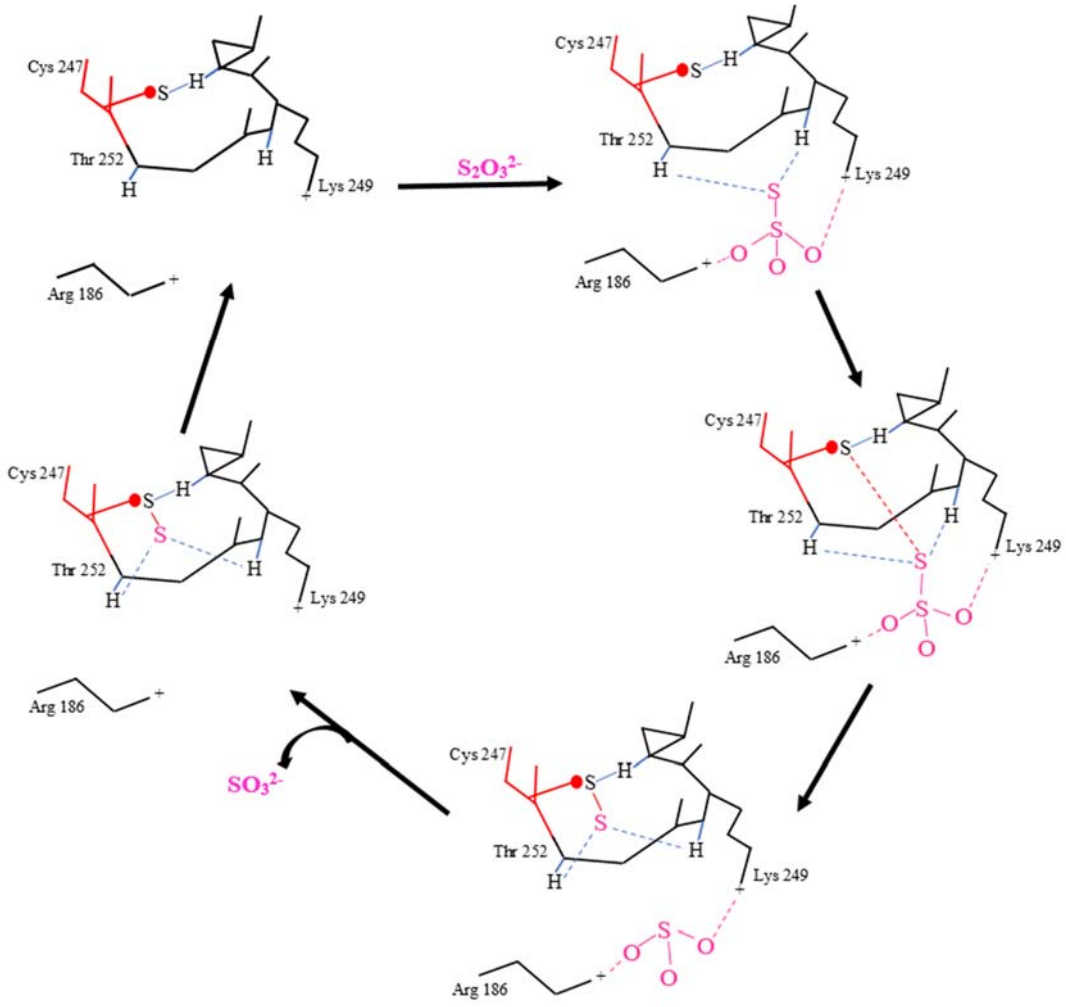

Figure 5. Double Displacement Mechanism of Rh (Step 1). The active site is the sulfhydryl group of Cys 247. The sulfur atom from the SD binds to the active site by forming a persulfide linkage. The persulfide intermediate is then stabilized by other amino acids around it.[40]

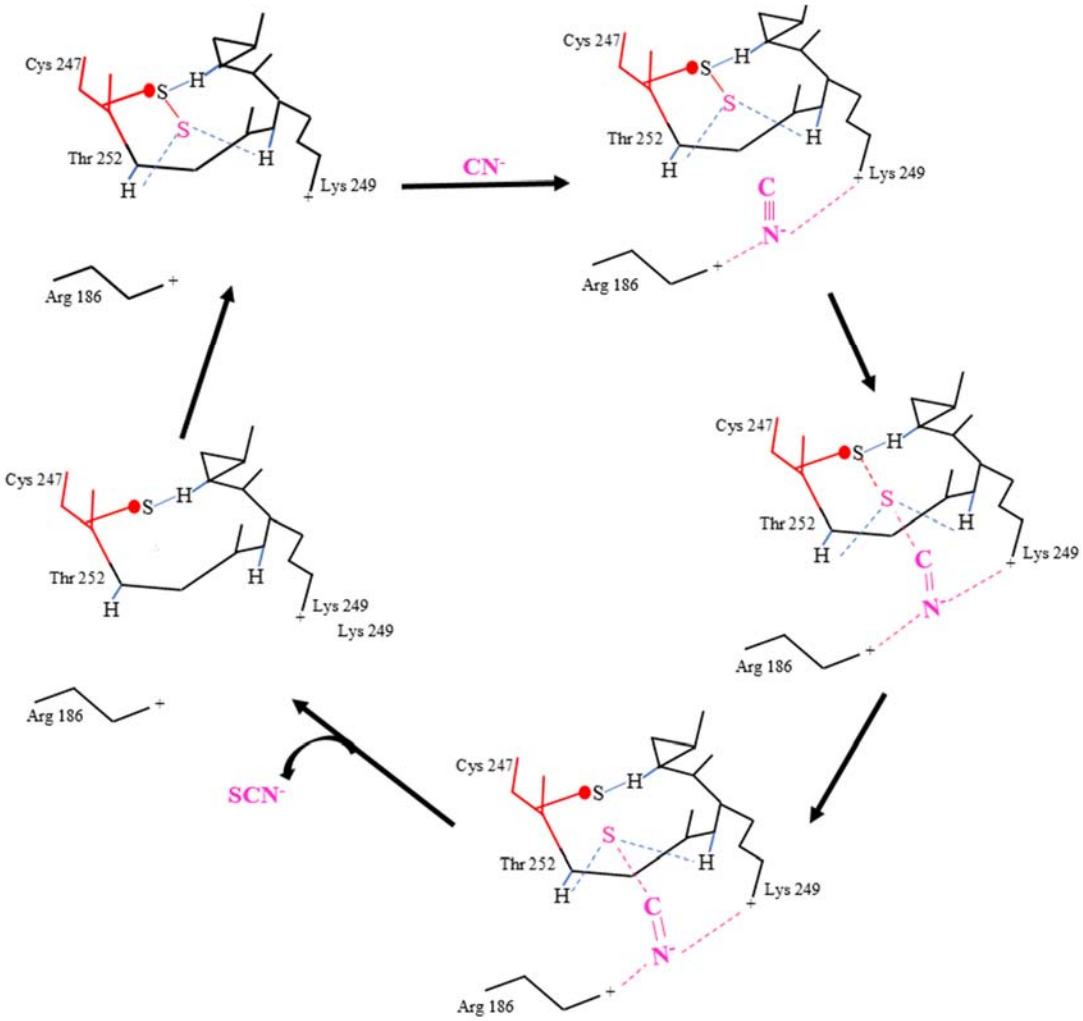

Figure 6. Double Displacement Mechanism of Rh (Step 2). At the active site, the bound sulfur atom is transferred to the CN^- to form SCN^-.[40]

Rh can employ a range of sulfane sulfur molecules, most commonly the inorganic thiosulfates.[41] The rate limiting factor for this catalytic reaction is the concentration of the SD. The Rh activity is inhibited by phosphate ions and divalent anions by interacting with the active site of the enzyme.[42]

PART 2

The ongoing projects in Dr. Petrikovics's lab include storage stability, particle size distribution, DMTS blood brain barrier penetration and *in vitro* SD efficacy studies. The *in vivo* studies include antidotal efficacy-, pharmacokinetic- and organ distribution studies. For the pharmacokinetic studies, blood DMTS concentrations need to be determined. An HPLC-UV-Vis detector was being used to quantify the DMTS in blood at concentrations higher than 1µg/mL. It was important to develop a sensitive method to detect low concentrations of DMTS below 1 µg/mL. Therefore, a fluorescence detection method was developed as a more sensitive method to determine low DMTS concentrations.

Fluorescence and Fluorescent probes

History of Fluorescence

Fluorescence and phosphorescence represent common types of photoluminescence.[43] The term "luminescence" is derived from the Latin word "lumen" = light. It was first introduced as "luminescenz" by the German physicist Eilhard Wiedemann in 1888.[43] There are different types of luminescence based on their mode of excitation such as chemiluminescence, bioluminescence and photoluminescence. Photoluminescence is the emission of light arising "from direct photoexcitation of the emitting species.[44] Fluorescence, phosphorescence, and delayed fluorescence can be considered as the common types of photoluminescence.[43] The term fluorescence was first introduced by Sir George Gabriel Stokes in the 19th century.[45] G.G Stokes carried out his experiments using both organic (quinine) and inorganic (fluorite) compounds and identified the common phenomenon called "dispersive reflection", which can be observed when the wavelength

of the dispersed light is longer than the wavelength of the original light. Later this became known as the Stokes Law.[43]

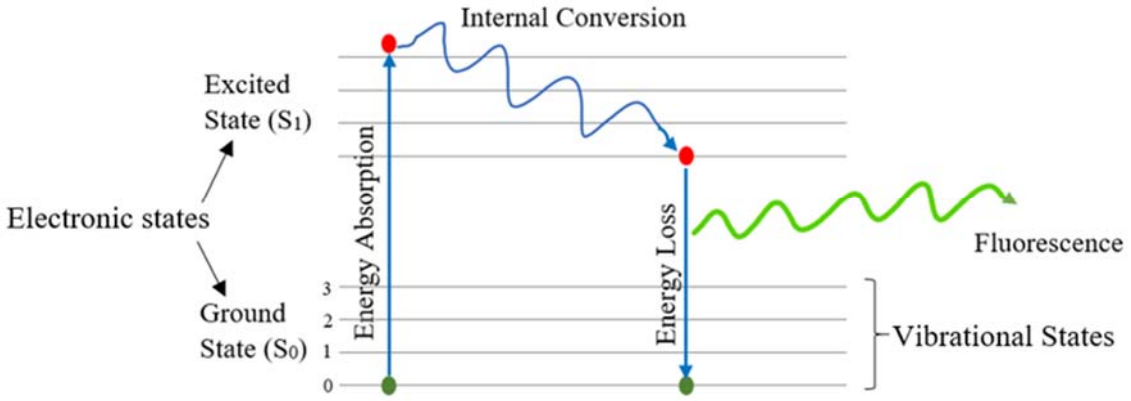

Figure 7. A Typical Jablonski Diagram.

A typical Jablonski diagram has shown in the figure 7. The singlet ground state and first excited state is denoted by the S_0 and S_1 respectively. The fluorescently active molecules can stay in any vibrational energy levels denoted by the 0, 1, 2, and 3. The vertical lines represent the energy transfer between two energy levels. The fluorescence process can be divided into three steps: a fluorescently active molecule can absorb a photon resulting in excitation of an electron to a higher vibrational level of the excited electronic state S_1. Collisions with other molecules can cause the loss of vibrational energy from the excited molecule. Then it rapidly relaxes to a lower vibrational state of S_1 which is called as internal conversion. When the molecule returns to the ground state S_0, it typically relaxes to a higher vibrational state S_0 in the ground electronic state while emitting a photon. The emitted photon has lower energy than the excited photon. Moreover, the emitted photon has longer wavelength than the excited photon.[46]

Fluorophores

A chemical probe is a small molecule that is used to study a component of a biological system such as a cell or an organism by reversibly binding to a target molecule.[47] In fluorescence spectroscopy, the fluorophore is the component that is responsible for absorbing light of a specific wavelength and emitting light at a different wavelength. The intensity of the both lights depend on the fluorophore and the chemical environment around it.[46] There are two types of fluorophores, intrinsic and extrinsic. Intrinsic fluorophores occur originally in the sample being studied. In biological systems aromatic amino acids, certain neurotransmitters, porphyrins, and green fluorescent protein are examples of intrinsic fluorophores. Extrinsic fluorophores do not occur originally in the system under study but are introduced into the sample by the experimenter.[46] They are added to the sample to provide fluorescence, or to change the spectral properties of the sample. Examples include dansyl group introduction and the formation of fluorescein and rhodamine.[46]

The fluorophores have unique absorption and emission spectra. In a typical (emission) fluorescence spectrum the excitation wavelength is fixed and the emission as a function of wavelength is measured. While in an excitation spectrum measurement, the emission wavelength is fixed and the excitation wavelength is varied. In a contour map, both excitation and emission is measured along with the emission intensities.

Sulfane Sulfur Probe 4 (SSP4) as a Sulfur Probe to Form Fluorescein to Detect Low Concentrations of DMTS

SSP4 (3',6'-Di(*O*-thiosalicyl) fluorescein) is a commercially available sulfane sulfur probe that selectively binds to the sulfane sulfur molecules.[48] SSP4 itself is non-

fluorescent. Once it reacts with a sulfane sulfur molecule, it produces fluorescein and benzodithiolone[48] (Figure 8). Fluorescein is not sensitive to solvent polarity.[46] Additionally, it possesses a high molar extinction coefficient of 80,000 M^{-1} cm^{-1}.[46]

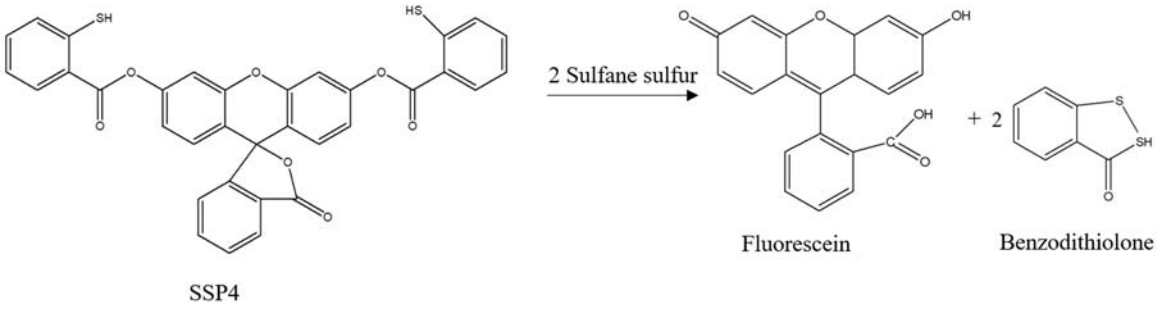

Figure 8. Chemical Reaction of SSP4 with Sulfane Sulfur Molecules. (http://www.dojindo.com/store/p/952-SulfoBiotics-SSP4.html)

SSP4 can be used for qualitative and quantitative analysis of the sulfane sulfurs. In this study, SSP4 was used to monitor the low concentrations of DMTS (below 1 μg/mL) in blood samples. The intensity of the fluorescent produced from the reaction can be measured using fluorescence detectors.

CHAPTER II

MATERIALS AND METHODS

Chemicals, Enzyme and Blood

Commercially available and highly purified chemicals were used for all experiments. DMTS, fluorescein and KCN were purchased from Sigma-Aldrich (Milwaukee, WI, USA); SD1 and iron (III) nitrate nonahydrate were purchased from Sigma-Aldrich (St. Louis, MO, USA); SD3 was purchased from Alfa Aesar (St. Louis, MO, USA). Acetonitrile (ACN) and water for HPLC were purchased from Acros Organics (Thermo Fisher Scientific, Geel, Belgium). Sulfane sulfur probe 4 (SSP4) was purchased from Dojindo Molecular Technologies, Inc. (Rockville, MD, USA). Rhodanese (bovine liver Type II, essentially salt-free, lyophilized powder, 100 units/mg) was purchased from Sigma-Aldrich (St. Louis, MO, USA). Citrated bovine blood was purchased from Carolina Biological Supply Company (Burlington, NC, USA).

Animals

Male CD-1 mice (Charles River Laboratories, Inc., Wilmington, Massachusetts, USA) were used for the *in vivo* efficacy studies and kept in a light and temperature-controlled room (22℃) with a 12-hour light and dark full-spectrum constant lighting cycle. Mice were fed with water and 4% Rodent Chow (Harlan Laboratories Inc., Indianapolis, Indiana, USA) ad libitum. Animal procedures were conducted according to the guidelines in "The Guide for the Care of Laboratory Animals" (National Academic Press, 2011) which are accredited by the Association for Assessment of Laboratory Animal Care, International. Surviving animals were terminated at the end of the experiments according to the American Veterinary Medical Association Guidelines. Experiments were approved

by the Institutional Animal Care and Use Committee (IACUC) at Sam Houston State University (IACUC Permission number: 15-09-14-1015-3-01).

Instruments

The following instruments were used for analysis (Table 1).

Table 1

Instruments used for the Research

Instruments	Brand and Model
HPLC	Thermo Scientific Dionex Ultimate 3000
UV Detector	Thermo Scientific Dionex VWD-3000
FLD Detector	Thermo Scientific Dionex FLD-3000
Fluorescence Spectrophotometer	HITACHI F-4500
UV-Vis Spectrophotometer	GENESYS^{TM} 10 UV series spectrophotometer

Method

PART 1

Determination of SD Efficacies *In Vitro at pH 7.4 and 8.6*

The *in vitro* abilities of SD_1, SD_2 and SD_3 to convert CN^- into SCN^- were measured at pH 7.4, and pH 8.6 using the spectrophotometric method of Westley with minor modifications.[14]

Preparation of 250 mM KCN Solution

Using an analytical scale, 1.6288 g of KCN was measured into a VWR glass bottle. One hundred milliliters of water was added. The mixture was hand vortexing until the KCN had dissolved completely.

Preparation of SD Solutions (SD_1, SD_2 and SD_3)

SD_1 (0.0919 g) was measured using an analytical balance and dissolved in 10 mL of water in a glass vial to prepare a 30 mM stock solution. The solution was then mixed by hand vortexing. SD_1 solutions (10, 15, 20 and 25 mM) were prepared by diluting the 30 mM stock solution in glass tubes. SD_2 (0.0631 g) was measured using an analytical balance and dissolved in 10 mL of ethanol in a glass vial to prepare a 50 mM stock solution. The solution was then mixed by hand vortexing. SD_2 solutions (10, 20, 30 and 40 mM) were prepared by diluting the 50 mM stock solution in glass vials. SD_3 (0.3953 g) was measured using an analytical balance and dissolved in 10 mL of water in a glass vial to prepare a 250 mM stock solution. The solution was then mixed by hand vortexing. SD_3 solutions (125, 150, 175 and 200 mM) were prepared by diluting the 250 mM stock solution in glass vials.

Preparation of 100 unit/mL Rh Solution

Rh (1 mg, 100 units/mg) was dissolved in 1 mL of pH 7.4 phosphate buffer (10 mM) in a plastic eppendorf tube in order to prepare a Rh solution at pH 7.4. Rh (1 mg, 100 units/mg) was dissolved in 1 mL of pH 8.6 phosphate buffer (10 mM) in a plastic eppendorf tube to prepare a Rh solution at pH 8.6. Both were stored at 4℃.

Spontaneous Conversion of CN^- into SCN^- at pH 7.4

The purpose of this study was to determine the SD efficacy (CN conversion efficacy) of SD_1, SD_2 and SD_3 in the absence of Rh at pH 7.4 (physiological pH in the body). The spectrophotometric thiocyanate assay of Westley was carried out.[14] Water (400 µL), phosphate buffer (200 µL of 10 mM, pH=7.4), KCN (200 µL of 250 mM) and SD_1 solution (200 µL) (one concentration at one time) were added into the test tube (1) (Figure 9). The test tube was immediately vortexed and incubated for 1 minute at room

temperature. The reaction between the relevant SD and CN^- was then stopped by adding formaldehyde (500 µL of 15%). CN^- reacts with formaldehyhde to produce a stable complex of cyanohydrin which stops further reaction of CN^- and SD. Ferric nitrate solution ($Fe(NO_3)_3$) (1.5 mL of 40 mM) was added to the test tube in order to form the red colored ferric thiocyanate ($Fe(SCN)_3$) complex. The intensity of the colored complex was measured spetrophotometrically at 460 nm using a GENESYS^{TM} 10 UV series spectrophotometer. Three replicates were used for each set of initial concentrations. The same procedure was carried out for SD_2 and SD_3.

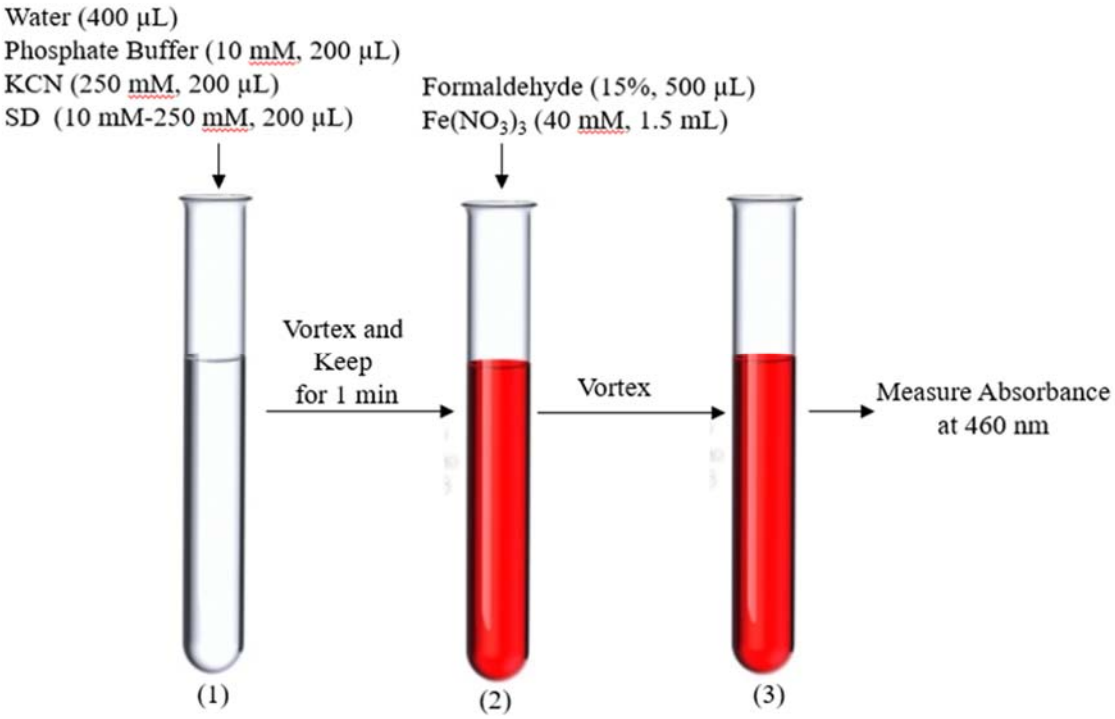

Figure 9. Spontaneous Conversion of CN^- into SCN^-. Formation of SCN^- within 1 minute was measured and expressed as SD efficacy. (1) CN^- was converted into SCN^- by the SD. (2) Formation of SCN^- was stopped by adding formaldehyde and upon the addition of $Fe(NO_3)_3$ the red colored $Fe(SCN)_3$ complex was produced. (3) Intensity of the red colored complex was measured by a GENESYS^{TM} 10 Series spectrophotometer at 460 nm.

Enzymatic Conversion of CN^- into SCN^- at pH 7.4 and 8.6

The purpose of this study was to determine the SD efficacy (CN^- conversion efficacy) of SD_1, SD_2 and SD_3 in the presence of Rh (1 unit/mL) at pH 7.4 (Physiological pH in the body) and pH 8.6 (optimum pH for Rh). The spectrophotometric thiocyanate assay of Westley was carried out.[14] Water (390 µL), phosphate buffer (200 µL of 10 mM, pH=7.4), KCN (200 µL of 250 mM), Rh (10 µL of 1 unit/mL) and SD_1 solution (200 µL) (one concentration at one time) were added into the test tube (1) (Figure 10). The test tube was immediately vortexed and incubated for 1 minute at room temperature. The reaction between the relevant SD and CN^- was then stopped by adding formaldehyde (500 µL of 15%). $Fe(NO_3)_3$ solution (1.5 mL of 40 mM) was added to the test tube in order to form the red colored $Fe(SCN)_3$. The intensity of the colored complex was measured spetrophotometrically at 460 nm using a GENESYS^{TM} 10 UV series spectrophotometer. Three replicates were used for each set of initial concentrations same procedure was carried out for SD_2 and SD_3.

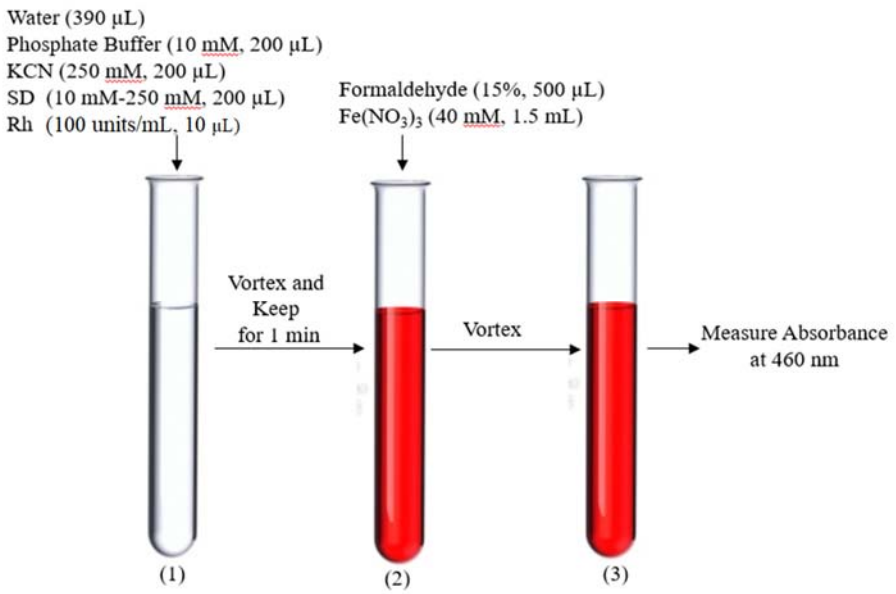

Figure 10. Enzymatic Conversion of CN^- into SCN^-. Formation of SCN^- within 1 min was measured and expressed as SD efficacy. (1) CN^- was converted into SCN^- by the SD. CN^- conversion was catalyzed in the presence of Rh. (2) Formation of SCN^- was stopped by adding formaldehyde and upon the addition of $Fe(NO_3)_3$ the red colored $Fe(SCN)_3$ complex was produced. (3) Intensity of the red colored complex was measured by using GENESYS^{TM} 10 Series spectrophotometer at 460 nm.

Calibration Curve for Thiocyanate

The purpose of this calibration curve was to quantify the relationship between the absorbance at 460 nm (for red colored $Fe(SCN)_3$ complex) and the amount of SCN^- formed (within 1 minute by the SDs) in the above experiments. $Fe(NO_3)_3.9H_2O$ (1.210 g) was measured using an analytical balance. It was transferred to a 10-mL volumetric flask and diluted with water up to the mark to prepare the $Fe(NO_3)_3.9H_2O$ solution (0.5 M). The solution was vortexed until the salt dissolved completely. KSCN (1.460 g) was measured using an analytical balance. It was transferred to a 10 mL volumetric flask and diluted with water up to the mark to prepare the KSCN (1.5 M) solution. The solution was vortexed until the salt dissolved completely. Both solutions were added (1:1 ratio) into a 20 mL

Erlenmeyer flask and vortexed to prepare a ferric thiocyanate solution (0.25 M). The solution was diluted with water to prepare ferric thiocyanate stock solution (2.5 mM). The stock solutions were diluted to make of $Fe(SCN)_3$ solutions (0, 0.083, 0.17, 0.33, 0.42, 0.50, 0.58, 0.67, 0.75, 0.92, 1.00 and 1.04 mM). Absorbance of each $Fe(SCN)_3$ solution was measured using a GENESYS^{TM} 10 Series spectrophotometer at 460 nm *vs.* SCN^- concentrations.

Determination of Antidotal Efficacy of Three Different SDs in Mice *In vivo*

Male CD-1 mice were injected with KCN solution via subcutaneous administration. The dose of KCN was determined based on the Dixon and Massey method.[15] Within one minute of the injection of KCN, the antidote SD_1, was administered IM into the rear right leg of each mice. After injection, the animals were kept in a cage for observation (alive or dead). If the animal was dead, the dose was decreased. If it was alive, the dose was increased. The process was continued until the stopping condition, which was determined by the Dixon and Massey method[15], was met. For the control, only KCN was injected and the same procedure was carried out until the stopping condition was met. At the stopping condition, a LD_{50} value was given by the Dixon and Massey method. The antidotal potency ratio (APR) was calculated for the antidote SD_1 based on the given LD_{50} values by the Dixon and Massey's method.

APR = (KCN LD_{50} with SD)/ (KCN LD_{50} without SD)

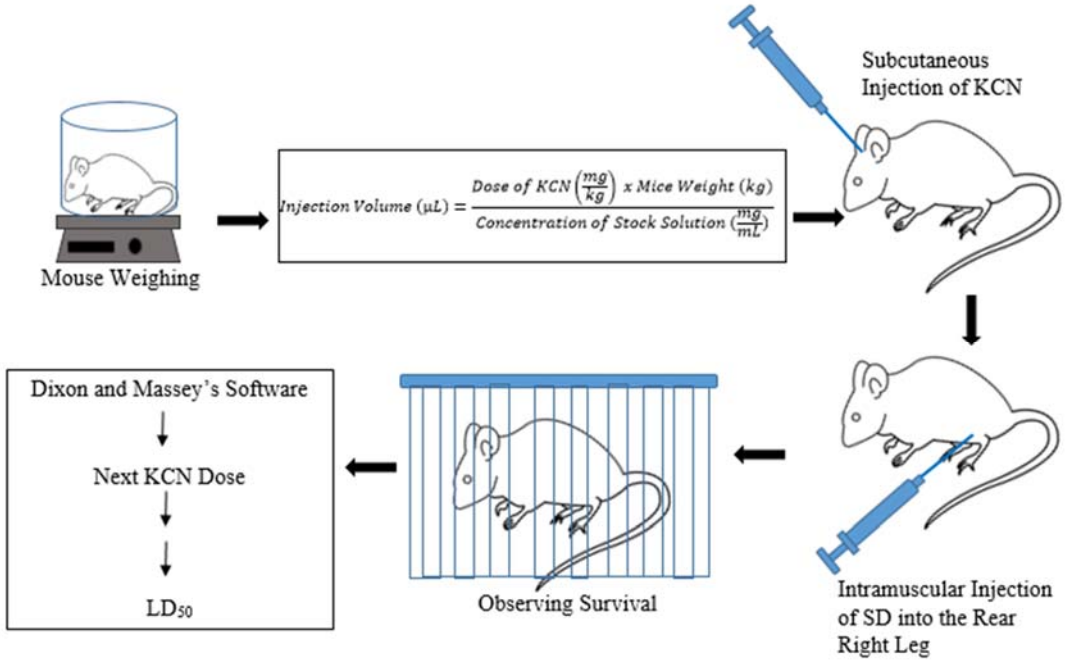

Figure 11. In Vivo Antidotal Efficacy Study Procedure. Weight of the mice was measured. Injection volume for both SD_1 and KCN was calculated based on the mice weight. KCN was injected subcutaneously and SD_1 was injected intramuscularly. Mice survival was observed after injections and recorded in the software. (http://www.wedrawanimals.com/how-to-draw-a-mouse/)

PART 2

Fluorescent Method Development for Measuring the Selected CN Antidote DMTS at Low Concentrations

Pharmacokinetic studies are being carried out in Dr. Petrikovics's Lab, where mice blood DMTS concentrations are needed to be determined. Therefore, the purpose of this experiment was to develop a rapid and sensitive analytical method to detect low concentrations of DMTS (below 1 µg/mL) in mice blood samples using fluorescence detector in HPLC. The SSP4 was used as an extrinsic fluorophore and added to the sample of DMTS to produce a fluorescently active molecule. As a preliminary study, a method was developed using a fluorescence spectrophotometer. Three-dimensional (3D) and two-

dimensional (2D) scanning studies were carried out to select the best excitation and emission wavelengths for the reaction mixture containing SSP4 and DMTS in ACN. In the second step, selected excitation and emission wavelengths were used to develop a method to detect low concentrations of DMTS in ACN using a fluorescence detector in HPLC. The same HPLC-Fluorescence detector method was used to detect low concentrations of DMTS/ACN in mice blood samples. The developed method using a fluorescence detector in HPLC is expected to be used in future pharmacokinetic studies.

Preparation of SSP4 Stock Solution

SSP4 (1 mg) was dissolved in dimethyl sulfoxide (DMSO) (660 µl) in a plastic vial by pipetting to prepare the SSP4 stock solution (2.5 mM). The stock solution was then aliquoted (10 µl volumes) into individual glass vials covered with aluminum foil. They were stored at -20℃ and used within two months.

Preparation of SSP4 Working Solution

The SSP4 stock solution (2.5 mM) was diluted by adding HPLC-grade water (0.5 mL) to prepare 50 µM SSP4 (30.23 µg/mL) working solutions.

Preparation of DMTS Stock Solutions

Different concentrations of DMTS solutions (0-1.0 µg/mL) were prepared in ACN in glass vials. ACN was selected as a DMTS solvent due to its ability to extract DMTS from different biological matrices prior to analysis.

3D Scan of the Reaction Mixture Containing SSP4 and DMTS in ACN using Fluorescence Spectrophotometer

SSP4 working solution (300 µL of 50 µM) was gently mixed with DMTS solution (3 mL of 1.0 µg/mL) in a 1.0 × 1.0 cm, 3 ml quartz cell. The reaction mixture was incubated

at room temperature for a few seconds in a dark container prior to analysis. The fluorescence spectrum was recorded on a HITACHI F-4500 fluorescence spectrophotometer. Due to the solvent effects on the absorption and emission spectra, the possible excitation wavelengths were selected by 3D scanning of the reaction mixture in the range of 200–900 nm. Excitation and emission sampling intervals were set to 10 nm. Scan speed was adjusted to 1200 nm/min. Excitation and emission slit widths were maintained at 5 nm. The photo-multiplier tube (PMT) voltage was adjusted to 700 V.

2D Scan of the Reaction Mixture Containing SSP4 and DMTS in ACN using Fluorescence Spectrophotometer

SSP4 working solution (300 µL of 50 µM) was gently mixed with DMTS solution (3 mL of 1.0 µg/mL) in the quartz cell. The reaction mixture was incubated at room temperature for few seconds in a dark container prior to analysis. The possible excitation wavelengths selected from the 3D scan were used to obtain the 2D spectra. The best emission wavelength was selected from the obtained 2D spectra and the best excitation and emission wavelengths were used for further analysis. A 2D fluorescence spectrum was recorded on a HITACHI F-4500 fluorescence spectrophotometer. Possible emissions were monitored in the range of 200-900 nm. Excitation and emission slit widths were maintained at 5 nm. The PMT voltage was adjusted to 700 V.

Calibration Curve to Determine Low Concentrations of DMTS in ACN using Fluorescence Spectrophotometer

Three mL of different concentrations of DMTS solutions (0, 0.1, 0.25, 0.4, 0.5 µg/mL) were prepared in ACN in glass vials. The SSP4 working solution (300 µL of 50 µM) was gently mixed with each DMTS solution. The reaction mixtures were incubated in

a quartz cell at room temperature for a few seconds in a dark container prior to analysis. The florescence spectrophotometer was set up to the best excitation and emission wavelengths (280/309 nm). Excitation and emission slit widths were maintained at 5 nm. The PMT voltage was adjusted to 700 V. Then, 2D scanning were run for each concentration of DMTS. The calibration curve was developed by plotting the fluorescence intensities *vs.* DMTS concentrations.

Calibration Curve to Determine Low Concentrations of DMTS in ACN using Fluorescence Detector in HPLC

Different concentrations of DMTS (0.025, 0.05, 0.1, 0.2, 0.4, 0.6, 0.8, 0.9 and 1.0 µg/mL) were prepared in ACN in glass vials. Aliquots of each DMTS solution (400 µL) were then diluted with ACN (200 µL) in plastic vials. SSP4 working solution (50 µL of 50 µM) were gently mixed with each diluted DMTS solution (500 µL). The mixture was incubated at room temperature for a few seconds in a dark container prior to analysis. The best excitation and emission wavelengths (280/309 nm) obtained from the fluorescence spectrophotometer were set up in a VWD-300 fluorescence detector in Dionex Ultimate 3000 HPLC system. The following HPLC conditions were used: column: a non-polar Luna® C-8(2) analytical column (250 × 4.6 mm, pore size of 100Å, 5 µm particle sizes, Phenomenex Inc., Torrance, CA), column temperature: 25 ˚C, injection volume: 100 µL, mobile phase: water: acetonitrile (35%: 65%) isocratic elution for 25 min, flow rate: 1.0 mL/min. The calibration curve was developed by plotting the peak area *vs.* DMTS concentrations in ACN.

Calibration Curve to Determine Low Concentrations of DMTS/ACN in Blood Samples using Fluorescence Detector in HPLC

Different concentrations of DMTS (0.025, 0.05, 0.1, 0.2, 0.4, 0.6, 0.8 µg/mL) were prepared in ACN in glass vials. Aliquots of whole bovine blood (200 µL) was spiked with DMTS (400 µL). The mixture was hand vortexed immediately followed by centrifugation for 5 minutes at 13000 RCF at 4℃. The supernatant (500 µL) was collected and mixed with SSP4 working solution (50 µL of 50 µM). The mixture was incubated at room temperature for few seconds in a dark container prior to analysis. The best excitation and emission wavelengths (280/309 nm) obtained from the fluorescence spectrophotometer were set up in a VWD-300 fluorescence detector in Dionex Ultimate 3000 HPLC system. The following HPLC conditions were used: column: a non-polar Luna® C-8(2) analytical column (250 × 4.6 mm, pore size of 100Å, 5 µm particle sizes, Phenomenex Inc., Torrance, CA), column temperature: 25 ℃, injection volume: 100 µL, mobile phase: water: acetonitrile (35%: 65%) isocratic elution for 25 min, flow rate: 1.0 mL/min. The calibration curve was developed by plotting the peak area *vs.* DMTS concentrations in the blood samples.

CHAPTER III

RESULTS AND DISCUSSION

PART 1

Determination of SD Efficacy of Three Different SDs using a Spectrophotometric SCN Assay *In Vitro* at pH 7.4 and pH 8.6

SD efficacy (CN^- conversion efficacy) of SD_1, SD_2 and SD_3 were monitored *in vitro* at pH 7.4 (spontaneous conversion of CN^-) and at pH 7.4 and 8.6 (enzymatic conversion of CN^-). Different concentrations of SD_1 (0, 10, 15, 20, 25 and 50 mM), SD_2 (0, 10, 20, 30, 40 and 50 mM) and SD_3 (0, 125, 150, 175, 200 and 250 mM) solutions were added to KCN (250 mM) solution to produce SCN^-. The amount of SCN^- formed within 1 minute by each reaction was measured and recorded as an average rate and ± standard deviation (*s*). The color intensity of $Fe(SCN)_3$ upon the addition of $Fe(NO_3)_3$ was measured spectrophotometrically at 460 nm according to the standard protocol of the spectrophotometric thiocyanate assay of Westley. According to the standard protocol the reactions involved in the experiment can be summarized as follows:

$$CN^- + SD \rightarrow SCN^-$$

$$Fe^{3+} + 3SCN^- \rightarrow Fe(SCN)_3$$

Figure 12. $Fe(SCN)_3$ Formation Reaction. CN^- is converted to SCN^- by utilizing [s] in SD. $Fe(SCN)_3$ is formed upon addition of $Fe(NO_3)_3$.

The amount of SCN^- formed was calculated from the absorbance of $Fe(SCN)_3$ for each SD using the equation of the calibration curve for absorbance *vs.* concentration of SCN^-. Then, the SD efficacy was expressed as follows:

$$SD\ Efficacy = \frac{Change\ in\ Concentration\ of\ SCN^-\ \ (mM)}{1\ minute}$$

The calibration curve was developed by plotting the absorbance at 460 nm *vs.* $Fe(SCN)_3$ concentrations.

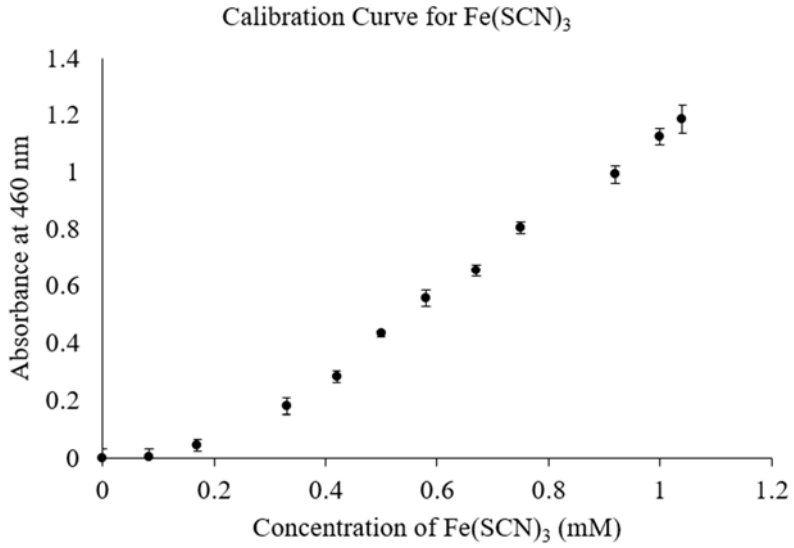

Figure 13. Calibration Curve for $Fe(SCN)_3$ Measured using UV Spectrophotometer. Data are presented as mean ± *s*; number of measurements (n) =3. Some error bars are not visible as the *s* is low.

$Fe(SCN)_3$ concentrations between 0.33 mM to 1.04 mM gave a good linear correlation with the absorbance at 460 nm. Therefore, linear range of the calibration curve was selected to calculate the SCN^- concentrations.

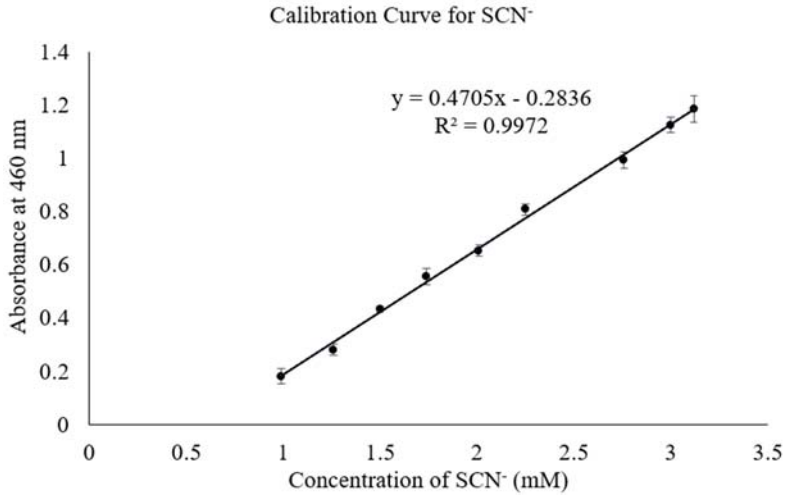

Figure 14. Calibration Curve for SCN^-. Data are presented as mean ± *s*; number of measurements (n) =3. Some error bars are not visible as the *s* is low.

The resulting linear plot, shown in figure 14 had an R^2 value of 0.9972 and an equation of y = 0.4705x - 0.2836.

The limit of detection (LOD) and limit of quantification (LOQ) were determined for the SCN^- calibration curve.

$LOD = y_{blank} + 3s = 0.0017 + (3 \times 0.03) = 0.09$

$Concentration\ LOD = 3s/\ m = (3 \times 0.03)/0.4705 = 0.19\ mM$

$0.19\ mM + X_{predicted} = 0.19\ mM + 0.60\ mM = 0.79\ mM$

$LOQ = y_{blank} + 10s = 0.0017 + (10 \times 0.03) = 0.60$

$Concentration\ LOQ = 10s/\ m = (10 \times 0.03)/\ 0.4705 = 0.64\ mM$

$0.64\ mM + X_{predicted} = 0.64\ mM + 0.60\ mM = 1.24\ mM$

Where y_{blank} is the mean of the blank signal, $X_{predicted}$ is the concentration of SCN^- predicted using the calibration equation and *s* is the standard deviation of the signal for the lowest analyzed concentration and *m* is the gradient of the calibration curve.

$s = \sqrt{\frac{(x_m - x_i)^2}{n-1}}$ where x_m is the mean of the repeats, x_i is the individual value of measurement and n is the number of repeats for the lowest analyzed concentration.

The accuracy (%) and precision (%) values for the SCN^- calibration curve are shown in table 2. Accuracy is nearness to the truth (% error) and precision is how well replicate measurements agree with one another, usually expressed as a relative standard deviation.[49]

$$Accuracy\ \% = \frac{x_{\ predicted} - x_{\ measured}}{x_{\ measured}} * 100$$

$$Precision\ \% = \frac{Standard\ Deviation\ of\ Absorbance}{Average\ Absorbance} * 100$$

Where $X_{predicted}$ is the concentration of SCN^- predicted using the calibration equation (Figure 14). $X_{measured}$ is the Concentration of SCN^- measured.

Table 2

The Accuracy (%) and Precision (%) for the Calibration Curve of SCN^-

Concentration of SCN^- (mM)	**Accuracy (%)**	**Precision (%)**
0.99	-0.36	16.57
1.26	-4.76	7.11
1.50	1.54	6.93
1.74	2.56	3.60
2.01	-0.96	1.53
2.25	3.02	3.72
2.76	-9.39	2.24
3.00	-7.29	1.95
3.12	0.04	0.53

Comparison of *in vitro* efficacy of the three SDs is shown in figure 15. The SD efficacy *vs.* SD concentrations gave good correlations with R^2 values within the range of 0.98-0.99.

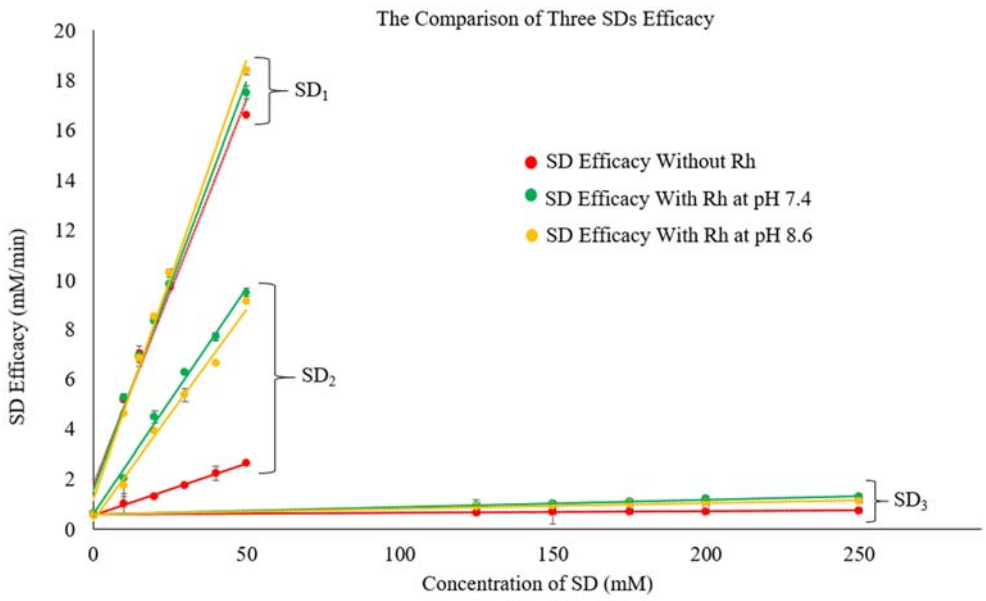

Figure 15. The Comparison of Different SD Efficacy *In Vitro*. Data are presented as mean ± *s*, n = 3. Some error bars are not visible as the *s* is low.

Intraday and interday accuracy (%) and precision (%) values are shown in table 3.

Table 3

Intraday and Interday Accuracy (%) and Precision (%) for the Comparison of Different SD Efficacy In Vitro

Concentration of SD (mM)		**Day 1**		**Day 2**	
		Accuracy (%)	Precision (%)	Accuracy (%)	Precision (%)
SD_1	15	8.29	1.90	6.22	1.49
	25	1.28	1.88	-2.26	2.00
	50	-1.17	2.61	-1.47	0.33
SD_2	50	-0.61	2.63	2.06	1.58
SD_3	150	34.17	0.82	-8.00	11.25
	200	0.63	0.57	-7.67	2.06
	250	-19.50	0.54	4.53	4.79

Determination of Antidotal Efficacy of SD_1 in Mice *In Vivo*

The purpose of this experiment was to determine the LD_{50} values with 95% confidence intervals for KCN in therapeutic mouse models. Mice received KCN solution subcutaneously and within 1 minute the SD_1 solution was administered IM. Different concentrations of KCN solutions were prepared in order to keep the injection volume below 200 µL. When the required CN dose was around 10 mg/kg, the stock solution with a lowest KCN concentration (2.5 mg/mL) was used. When the required CN dose was higher, the stock solution with a higher KCN concentration (5 or 7.5 mg/mL) was used. The formula below was used to determine the injection volume for each injection.

$$Injection\ Volume\ (\mu L) = \frac{Dose\ \left(\frac{mg}{kg}\right) x\ Animal\ Weight\ (g)}{Concentration\ of\ Stock\ Solution\ (\frac{mg}{mL})}$$

The dose of the SDs were held constant at 100 mg/kg body weight. According to the Dixon and Massey's up and down method, the applied CN doses were changed for each stage of each group. After adjusting the starting dose and the step size (dose difference between steps) for each group, next dose for each step was calculated. The next dose was based on the mortality results for the given step (Figure 16 and 17).

To meet the stopping condition criteria (four reversals of the doses), these experiments required 5 steps for the control (KCN alone). In the presence of the SD being tested, the number of steps depends on how far the initial CN dose is from the LD_{50} value.

The animals were observed for 1 hour and periodically for 24 hours after CN exposure for mortality. No toxic effects attributable to SD_1 were recorded in any of the mice at the doses used.

The *in vivo* data is shown below only for the control and SD_1.

Table 4

Determination of In Vivo Antidotal Efficacy of SD_1 in Mice.

Stage	Group	Mouse Weight (g)	KCN Dose (mg/kg)	SD_1 Dose (mg/kg)	KCN Volume (µL)	SD_1 Volume (µL)	Observation
1	Control	33	9		60 (C)		Live
	SD_1	32	20	100	85 (B)	64	Live
2	Control	33	11.5		76 (C)		Live
	SD_1	32	25	100	107 (B)	64	Dead
3	Control	32	14.5		93 (C)		Live
	SD_1	34	20	100	91(B)	68	Live
4	Control	38	18		91(B)		Dead
	SD_1	29	25	100	97 (B)	58	Dead
5	Control	30	14		84 (C)		Live
	SD_1	32	20	100	85 (B)	64	Live
6	Control	33	18		79 (B)		Dead
	SD_1	30	25	100	100 (B)	60	Dead
7	Control	31	14		85 (C)		Live
	SD_1		-	-			
8	Control	37	18		89 (B)		Dead
	SD_1		-	-			
9	Control	36	18		86 (B)		Dead
	SD_1		-	-			

(-) Indicates that the stopping condition was met. KCN solution used shown as (B) or (C).

Four working solutions of KCN were used (2.5, 5.0, 7.5, 10.0 mg/mL) for the study (Table 5). Different working solutions of KCN were used to prepare the KCN volume for an injection based on the KCN dose required. For higher doses, stock solutions with higher

KCN concentrations were used and, stock solutions with lower KCN concentrations were used for lower doses. A working solution of SD_1 (50 mg/mL) was used.

Table 5

Stock Solutions of KCN Prepared

Stock Solution of KCN	Concentration (mg/mL)
KCN - A	10.0
KCN - B	7.5
KCN - C	5.0
KCN - D	2.5

KCN and SD_1 volumes were calculated based on the formula below.

$$Injection\ Volume\ (\mu L) = \frac{Dose\ \left(\frac{mg}{kg}\right) x Animal\ Weight\ (g)}{Concentration\ of\ Stock\ Solution\ (\frac{mg}{mL})}$$

Injection volume calculations for KCN were done as follows:

For Stage 1:

Group 1: Control

KCN dose (9 mg/kg) was selected based on the Dixon and Massey's software. KCN working solution of 5.0 mg/mL was selected.

$$Injection\ Volume\ (\mu L) = \frac{9\left(\frac{mg}{kg}\right) x\ 33\ (g)}{5\ (\frac{mg}{mL})} = 60\ \mu L$$

Group 1: SD_1

KCN dose (20 mg/kg) was selected based on the Dixon and Massey's software. KCN working solution of 7.5 mg/mL was selected.

$$Injection\ Volume\ (\mu L) = \frac{20\left(\frac{mg}{kg}\right) x\ 32\ (g)}{7.5\ (\frac{mg}{mL})} = 85\ \mu L$$

SD_1 dose (100 mg/mL) was selected for all the stages. SD_1 working solution of 50.0 mg/mL was selected.

$$Injection\ Volume\ (\mu L) = \frac{100\left(\frac{mg}{kg}\right) x\ 32\ (g)}{50\ (\frac{mg}{mL})} = 64\ \mu L$$

All other calculations were done in the same way.

Figures 16 and 17 below show the screen shots of the user interface in Dixon and Massey's software for KCN and SD_1.

LD50 dose estimate:	16.240		Instructions for Using This Implementation of Dixon & Massey UDP, Introduction to Statistical Analysis, 1983, pgs 434-438.												
+95% confidence:	21.073														
-95% confidence:	12.514		1) enter initial dose into cell B18 and Log Step into cell B19												
Plus 95% log dose:	1.3237		2) Dose the animal at dose given at cell B21												
Minus 95% log dose:	1.0974		3) Enter an "L" or a "D" into cell C21 indicating outcome												
Log SEM:	0.0577		4) Repeat 2) & 3) at dose given in column B of next row												
Log LD50 estimate:	1.2106		5) continue until stopping condition (4 reversals) is met												
Consecutive Starts:	3		6) read LD50 dose and confidence limits from cells B2 ,B3, B4												
Initial Dose:	9.000		STOPPING CONDITION HAS BEEN MET										A table		C table
Log (dose)Interval:	0.1000														
Animal	Dose	Animal Lived (L) or Died (D)	Next Dose	Log_{10}(Dose)	Reversal? (0=no,1=yes)	consecutive from first reversal	Log_{10} of doses after (and immediately before) first reversal	Counted Died	Counted Lived	Graph X	Graph Y	N Lived - N Died	A	N Lived - N Died	one
1	9.000	l	11.330	0.9542	0	0				1	9	5	10.80	5	0.00
2	11.500	l	14.478	1.0607	0	0				2	11.5	4	7.72	4	0.00
3	14.500	l	18.254	1.1614	0	1	1.1614		1	3	14.5	3	5.22	3	0.00
4	18.000	d	14.298	1.2553	1	1	1.2553	1		4	18	2	3.20	2	0.00
5	14.000	l	17.625	1.1461	1	1	1.1461		1	5	14	1	1.53	1	0.00
6	18.000	d	14.298	1.2553	1	1	1.2553	1		6	18	0	0.00	0	0.00
7	14.000	l	17.625	1.1461	1	1	1.1461		1	7	14	-1	-1.55	-1	0.00
8	18.000	d	14.298	1.2553	1	1	1.2553	1		8	18	-2	-3.30	-2	0.00
1-Control															

Figure 16. The Screen Shot of the user Interface in Dixon and Massey's Software for Control

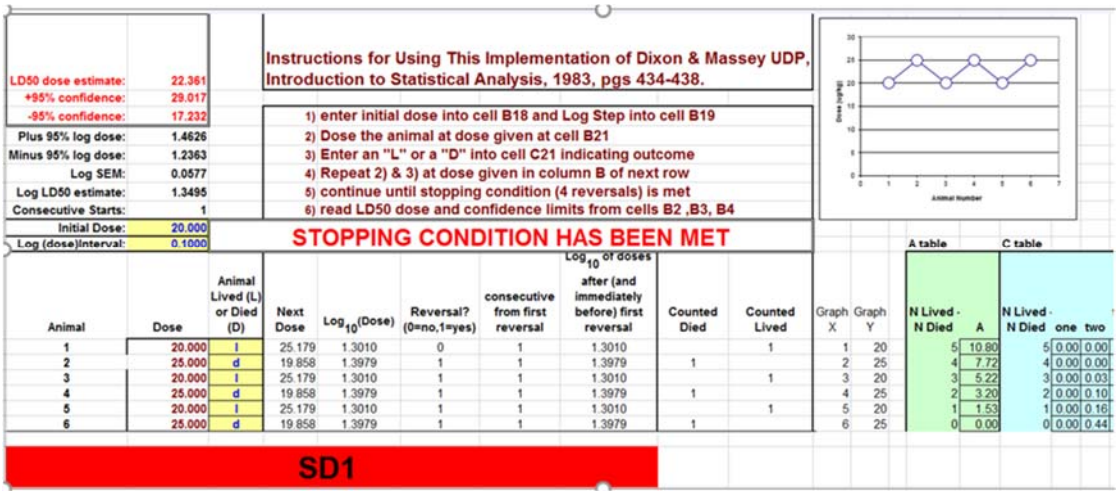

Figure 17. The Screen Shots of the user Interface in Dixon and Massey's Software for SD_1

Based on the LD_{50} obtained from the Dixon and Massey's software for both control and SDs, the APR value can be calculated using the following formula:

APR = (KCN LD_{50} with SD_1)/ (KCN LD_{50} without SD_1)

APR calculation for SD_1 has shown in Table 6.

Table 6

APR Value for SD_1

Group		LD_{50}	Confidence		APR
			+95%	-95%	
1	Control	16.24	21.07	12.51	-
2	SD_1	22.36	29.02	17.23	1.4

Comparison of APR values of three different SDs at the same dose of 100 mg/kg has shown below.

Table 7

Comparison of APR Values of Three Different SDs

Antidote	Dose of SD (mg/kg)	APR
SD_1	100	1.4
SD_2	100	3.2*
SD_3	100	1.1*

*Measured earlier by Dr. Petrikovics's team

PART 2

3D Scan of the Reaction Mixture Containing SSP4 and DMTS in ACN using Fluorescence Spectrophotometer

SSP4 (300 µL of 50 µM) and DMTS (3 mL of 1 µg/mL) were mixed in a quartz cell. The reaction mixture was incubated at room temperature for few seconds in a dark container. A 3D fluorescence spectrum was recorded on a fluorescence spectrophotometer. Possible excitations and emissions were monitored in the range of 200-900 nm.

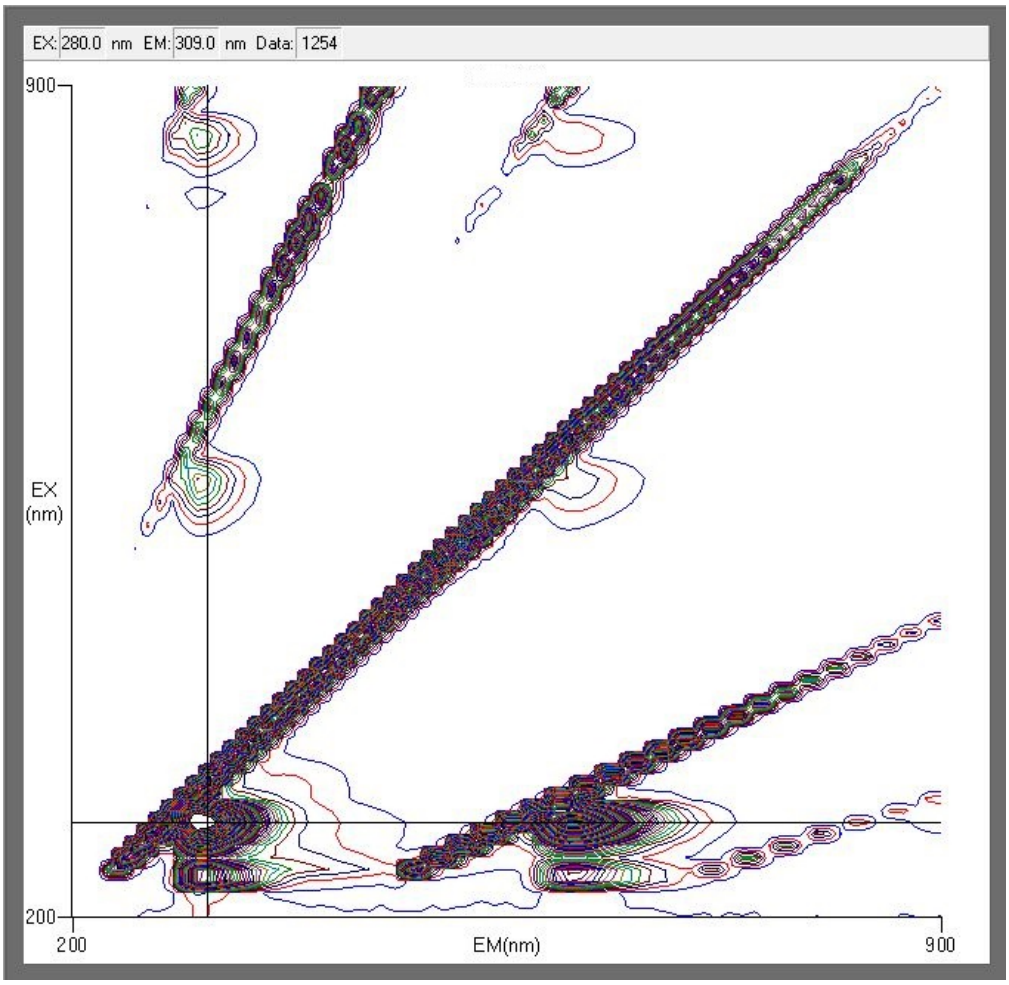

Figure 18. The Contour Plot of the Reaction Mixture of SSP4/Water (50 µM, 300 µL) + DMTS/ACN (1 µg/mL, 3 mL). Excitation at λ_{ex}=280 nm and λ_{ex}= 290 nm showed higher fluorescence intensity.

Two characteristic excitation and emission peaks for the reaction mixture containing SSP4 and DMTS were identified on the contour plot at $\lambda_{ex}/\lambda_{em}$ =280/309 nm, and $\lambda_{ex}/\lambda_{em}$ = 290/580 nm.

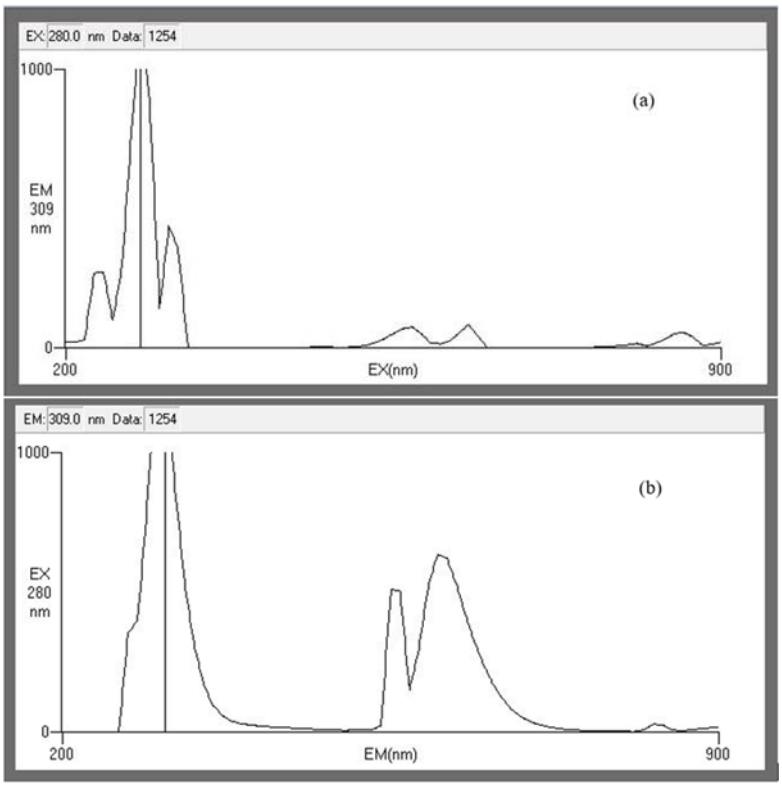

Figure 19. Excitation and Emission Plots for $\lambda_{ex}/\lambda_{em}$ =280/309 nm. (a) Emission plot shows higher excitation at 280 nm. (b) Excitation plot shows higher emission at 309 nm.

Table 8

Excitation and Emission Wavelength Values and their Intensities for the SSP4/Water + DMTS/ACN Reaction Mixture

Peak 1		**Peak 2**		**Rayleigh Scattering**	
$\lambda_{ex}/\lambda_{em}$ nm/nm	Intensity (a.u.)	$\lambda_{ex}/\lambda_{em}$ nm/nm	Intensity (a.u.)	$\lambda_{ex}/\lambda_{em}$ nm/nm	Intensity (a.u.)
280/309	1359	290/580	705.9	200/200-520/520	8.506-963.5
				530/530-700/700	866.7-207.8

The fluorescence intensity is much stronger when λ_{ex}=280 nm than 290 nm (1:1.93).

2D Scan of the Reaction Mixture Containing SSP4 and DMTS in ACN using Fluorescence Spectrophotometer

Reaction mixture of SSP4 in Water (50 µM, 300 µL) and DMTS in ACN (1 µg/mL, 3 mL) were excited at λ_{ex}=280 nm (Figure 20) and λ_{ex}= 290 nm (Figure 21) to obtain the 2D emission spectra.

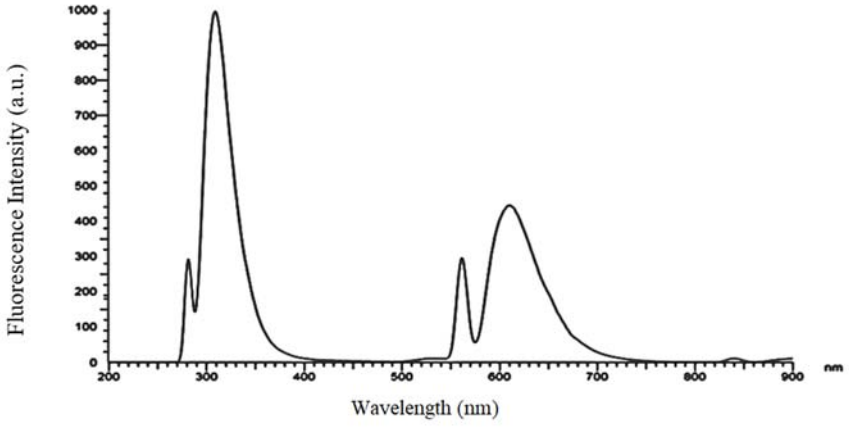

Figure 20. The 2D Spectrum of the Reaction Mixture of SSP4/Water (50 µM, 300 µL) + DMTS/ACN (1 µg/mL, 3 mL) at λ_{ex}=280 nm. Emission at λ_{em}=309 nm showed the highest fluorescence intensity.

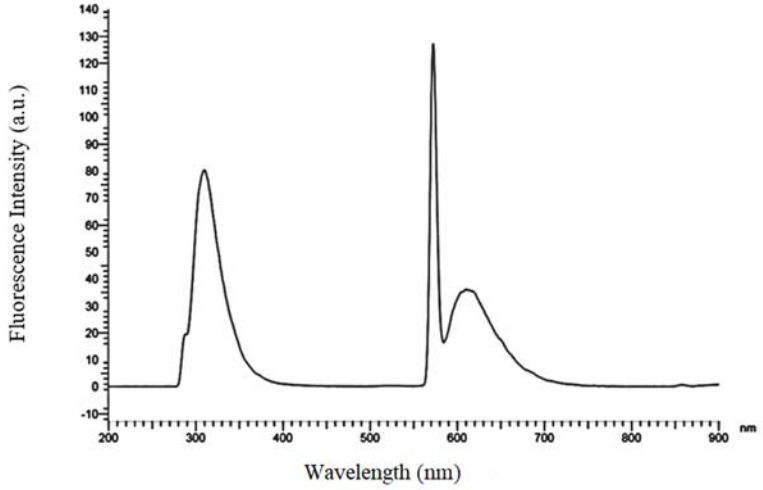

Figure 21. The 2D Spectrum of the Reaction Mixture of SSP4/Water (50 µM, 300 µL) + DMTS/ACN (1 µg/mL, 3 mL) at λ_{ex}=290 nm. Emission at λ_{em}=580 nm showed the highest fluorescence intensity.

The 2D spectrum of excitation at λ_{ex}=280 nm (Figure 20) showed the highest fluorescence intensity (~1000 a.u.) at λ_{em}=309 nm, while the 2D spectrum of excitation at λ_{ex}=290 nm (Figure 21) showed the highest fluorescence intensity (~130 a.u.) at λ_{em}=580 nm. Based on the fluorescence intensities of the contour plot and the 2D spectra, λ_{ex} /λ_{em}=280/309 nm were selected and used for further analysis as the best wavelengths to analyze the fluorescent product, yielded from the reaction between SSP4 and DMTS.

Dojindo Molecular Technologies, Inc., (commercial distributor of SSP4) has identified fluorescein as the main product of the reaction between SSP4 and sulfane sulfurs.[48] The fluorescein dye has absorption maxima from 480 nm to 600 nm and emission maxima from 510 nm to 610 nm.[46] The contour plot (Figure 18) indicated that the reaction between SSP4 and DMTS yields a fluorescent product which absorbs and emits at λ_{ex} /λ_{em}=280/309 nm with higher fluorescence intensity. Therefore, the fluorescent product yielded from the reaction between SSP4 and DMTS shouldn't be the fluorescein molecule.

Calibration Curve to Determine Low Concentrations of DMTS in ACN using Fluorescence Spectrophotometer

Five standard solutions of DMTS (0, 0.1, 0.25, 0.4, 0.5 µg/mL) were prepared in ACN and mixed with SSP4 (50 µM). 2D scans for each solution were run at λ_{ex} /λ_{em}=280/309 nm. The fluorescence intensity was evaluated for the fluorescent product formed from the reaction of SSP4 and DMTS in each solution at λ_{ex} /λ_{em}=280/309 nm. The calibration curve was developed by plotting the fluorescence intensity *vs.* DMTS concentrations in the range of 0-0.5 µg/mL.

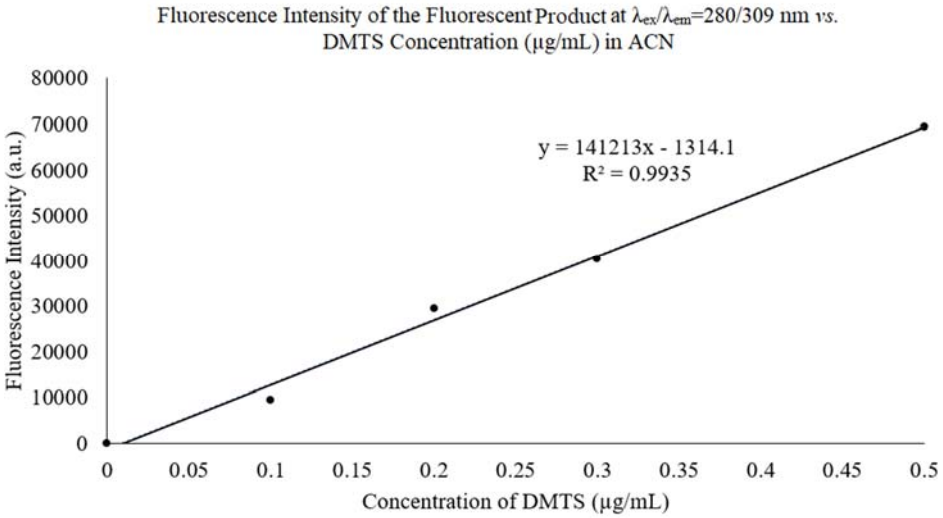

Figure 22. Calibration Curve for DMTS/ACN Measured using a Fluorescence Spectrophotometer. As a preliminary study, each data point was measured only once except the blank.

DMTS concentrations between 0 µg/mL to 0.5 µg/mL gave good correlation with the fluorescence intensity. The resulting linear plot, shown in figure 22, had an R^2 value of 0.9935 and an equation of y = 141213x - 1314.1.

The limit of detection (LOD) and limit of quantification (LOQ) were determined for the calibration curve.

$$LOD = y_{blank} + 3s = 637.81 + (3 \times 2539.02) = 8254.87$$

$$Concentration\ LOD = 3s/\ m = (3 \times 2539.02)/141213 = 0.05\ \mu g/mL$$

$$LOQ = y_{blank} + 10s = 637.8057 + (10 \times 2539.02) = 26028.01$$

$$Concentration\ LOQ = 10s/\ m = (10 \times 2539.02)/\ 141213 = 0.18\ \mu g/mL$$

Where y_{blank} is the mean of the blank signal, s is the standard deviation of the signal for the lowest analyzed concentration and m is the gradient of the calibration curve.

$s = \sqrt{\frac{\sum (y_{measured} - y_{predicted})^2}{n-2}}$ where $y_{measured}$ is the measured absorbance, $y_{predicted}$ is the predicted absorbance using the calibration equation.

The best excitation and emission values (λ_{ex} /λ_{em}=280/309 nm) obtained from the fluorescence spectrophotometer analysis were used to analyze the SSP4 and DMTS reaction mixture using a fluorescence detector in HPLC.

Calibration Curve to Determine Low Concentrations of DMTS in ACN using Fluorescence Detector in HPLC

DMTS (500 µL of 0.025, 0.05, 0.1, 0.2, 0.4, 0.6, 0.8, 0.9 and 1.0 µg/mL) in ACN were mixed with SSP4 (50 µL of 50 µM) in water. Excitation and emission wavelengths (λ_{ex}/λ_{em}=280/309 nm) obtained from the fluorescence spectrophotometer were used for the analysis of the fluorescent product in each DMTS solution using fluorescence detector in HPLC. The chromatogram for the reaction mixture of SSP4 and DMTS is shown below (Figure 23).

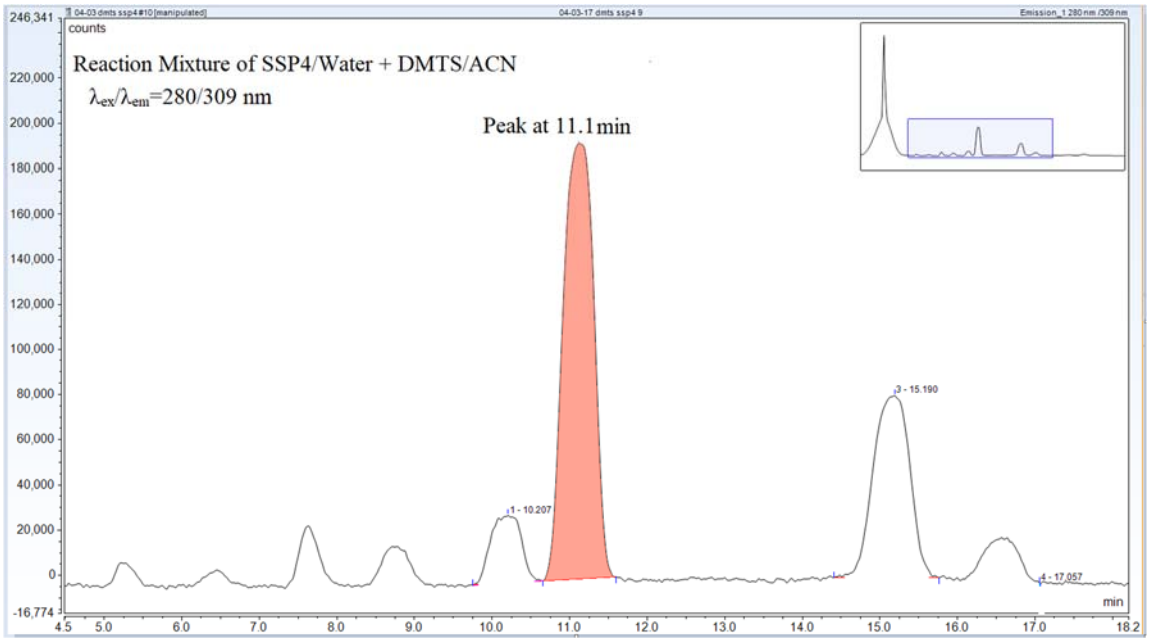

Figure 23. Chromatogram for the Reaction Mixture of SSP4/Water (50 µM, 50 µL and DMTS/ACN (1.0 µg/mL, 500 µL). The peak at 11.1 min showed the highest peak area for the quantification.

The chromatogram obtained for the reaction mixture of SSP4 and DMTS showed a peak at 11.1 min with significantly larger peak area compared to the other peaks. The peak showed a good proportionality with DMTS concentrations (Figure 24).

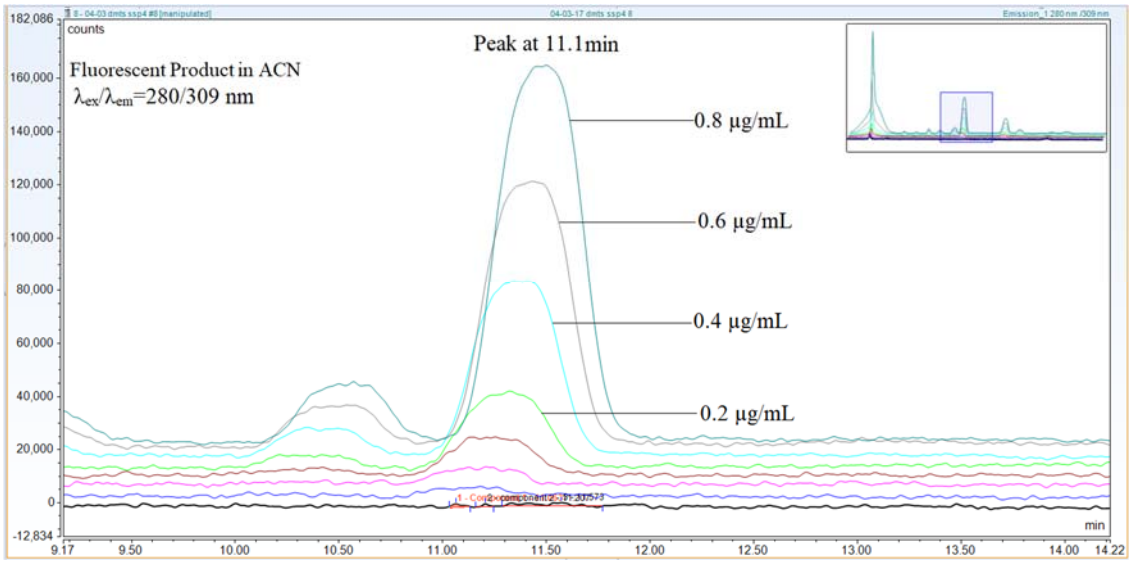

Figure 24. Proportionality of the Corresponding Peak for the Fluorescent Product at 11.1 min with DMTS Concentrations (0.025 – 0.8 µg/mL) in ACN.

Based on the chromatograms, the peak at 11.1 min was considered as the corresponding peak for the fluorescent product, yielded from the reaction between SSP4 and DMTS in ACN. Since, the peak at 11.1 min showed a good proportionality with DMTS concentrations, it was used to quantify the amount of DMTS in ACN originally present before the reaction.

The calibration curves were developed by plotting the peak area of the peak at 11.1 min *vs.* DMTS concentrations in ACN in the range of 0.025 – 1.0 µg/mL.

Two calibration curves were plotted by assuming the reaction of SSP4 and DMTS is 1:1 mole ratio (Figure 25) and 1:2 mole ratio (Figure 26).

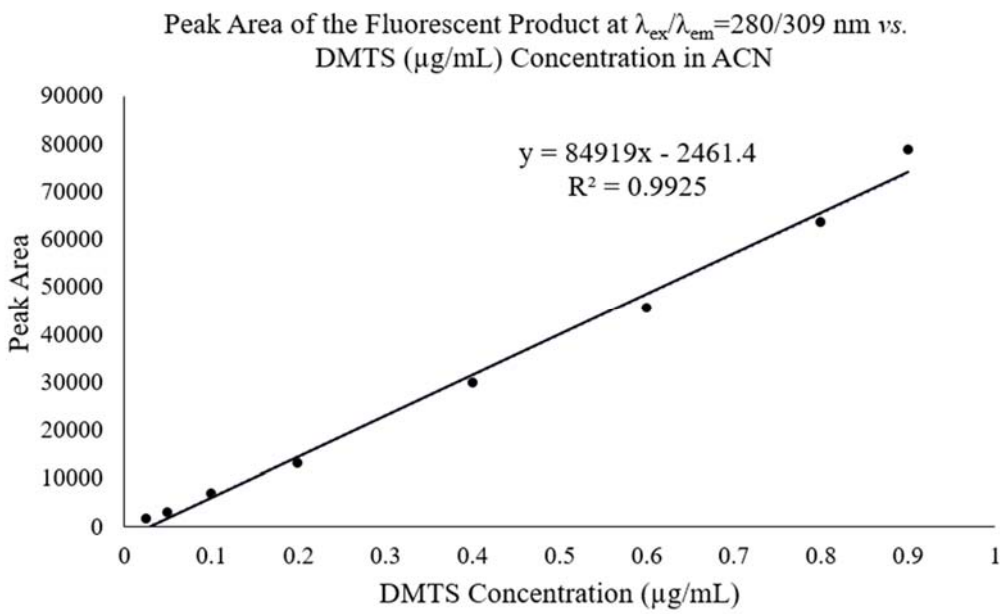

Figure 25. Calibration Curve for DMTS/ACN Measured using Fluorescence Detector in HPLC (SSP4: DMTS = 1:1). As a preliminary study, each data point was measured only once except the blank.

DMTS concentrations between 0.025 µg/mL to 0.9 µg/mL gave good correlation with the changes in fluorescence intensity when assume the reaction of SSP4 and DMTS is 1:1 mole ratio. The resulting linear plot, shown in figure 25, had an R^2 value of 0.9925 and an equation of y = 84919x – 2461.4.

The limit of detection (LOD) and limit of quantification (LOQ) were determined for the calibration curve.

$$LOD = y_{blank} + 3s = 38.62 + (3 \times 4.12) = 50.98$$

$$Concentration\ LOD = 3s/\ m = (3 \times 4.12)/84919 = 0.00015\ \mu g/mL$$

$$LOQ = y_{blank} + 10s = 38.62 + (10 \times 4.12) = 79.82$$

$$Concentration\ LOQ = 10s/\ m = (10 \times 4.12)/\ 84919 = 0.00049\ \mu g/mL$$

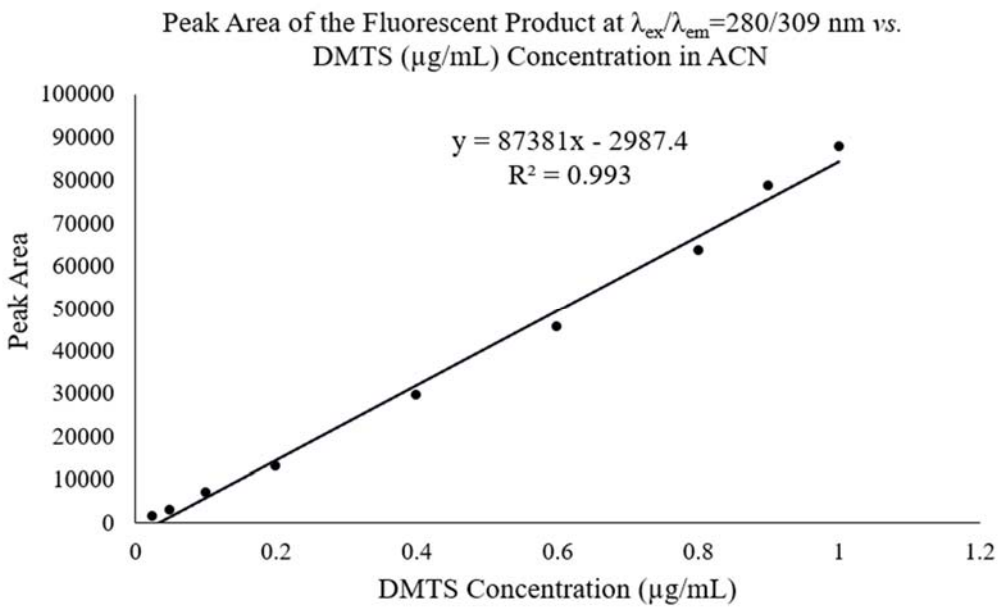

Figure 26. Calibration Curve for DMTS/ACN Measured using Fluorescence Detector in HPLC (SSP4: DMTS = 1:2). As a preliminary study, each data point was measured only once except the blank.

Different DMTS concentrations between 0.025 µg/mL to 1.0 µg/mL gave good correlation with the changes in fluorescence intensity when assume the reaction of SSP4 and DMTS is 1:2 mole ratio. The resulting linear plot, shown in figure 26, had an R^2 value of 0.993 and an equation of y = 87381x – 2987.4.

The limit of detection (LOD) and limit of quantification (LOQ) were determined for the calibration curve.

$$LOD = y_{blank} + 3s = 38.62 + (3 \times 4.12) = 50.98$$

$$Concentration\ LOD = 3s/\ m = (3 \times 4.12)/87381 = 0.00014\ \mu g/mL$$

$$LOQ = y_{blank} + 10s = 38.62 + (10 \times 4.12) = 79.82$$

$$Concentration\ LOQ = 10s/\ m = (10 \times 4.12)/\ 87381 = 0.00047\ \mu g/mL$$

Where y_{blank} is the mean of the blank signal, s is the standard deviation of the signal for the lowest analyzed concentration and m is the gradient of the calibration curve.

$s = \sqrt{\frac{(x_m - x_i)^2}{n-1}}$ where x_m is the mean of the repeats, x_i is the individual value of measurement and n is the number of repeats for the lowest analyzed concentration.

Accuracy (%) values for the calibration curve is shown in table 9.

Table 9

Intraday and Interday Accuracy (%) for the Calibration Curve of Peak Area vs. DMTS Concentration (µg/mL) in ACN

Concentration of DMTS (µg/mL)	**Accuracy (%)**	
	Day 1	**Day 2**
0.2	-8.1699	11.6163
0.4	-6.5861	-11.6161
0.6	-7.6813	3.8721

Calibration Curve to Determine Low Concentrations of DMTS/ACN in Blood Samples using Fluorescence Detector in HPLC

The calibration curve for the peak area at 11.1 min *vs.* DMTS concentrations in ACN showed a good linearity in the range of 0.025-1.0 µg/mL. Therefore, same HPLC-Fluorescent method was used to develop the calibration curve for low concentrations of DMTS/ACN in blood samples with SSP4. Different concentrations of DMTS (0.025, 0.05, 0.1, 0.2, 0.4, 0.6, 0.8 µg/mL) were prepared in ACN. Whole blood (200 µL) was spiked with DMTS (400 µL), then the mixture was hand vortexed and centrifuged. The supernatant (500 µL) was collected and mixed with SSP4 (50 µL of 50 µM) working solution. Excitation and emission wavelengths ($\lambda_{ex}/\lambda_{em}$=280/309 nm) obtained from the fluorescence spectrophotometer were used for the analysis of the fluorescent product in

each DMTS solution using fluorescence detector in HPLC. The chromatogram for the reaction mixture of SSP4 and DMTS is shown below (Figure 27).

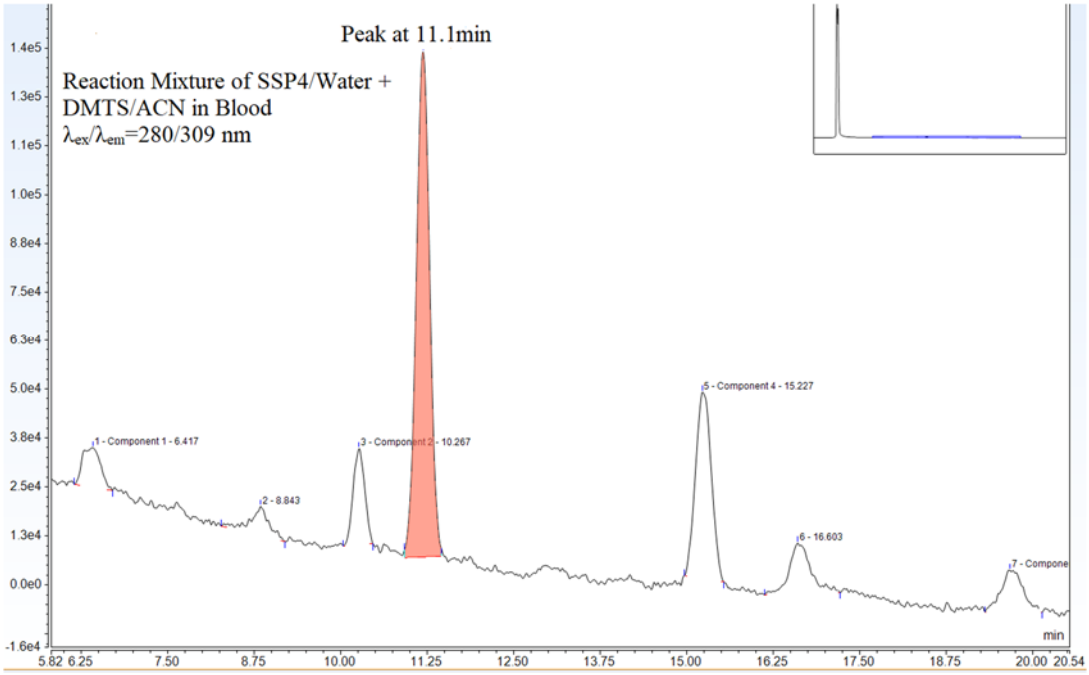

Figure 27. Chromatogram for the Reaction Mixture of SSP4/Water (50 µM, 50 µL and DMTS/ACN in Blood (0.8 µg/mL, 500 µL). The peak at 11.1 min showed the highest peak area for the quantification.

The chromatogram obtained for the reaction mixture of SSP4 and DMTS showed a peak at 11.1 min with significantly bigger peak area compared to the other peaks. The peak showed a good proportionality with DMTS concentrations (Figure 28).

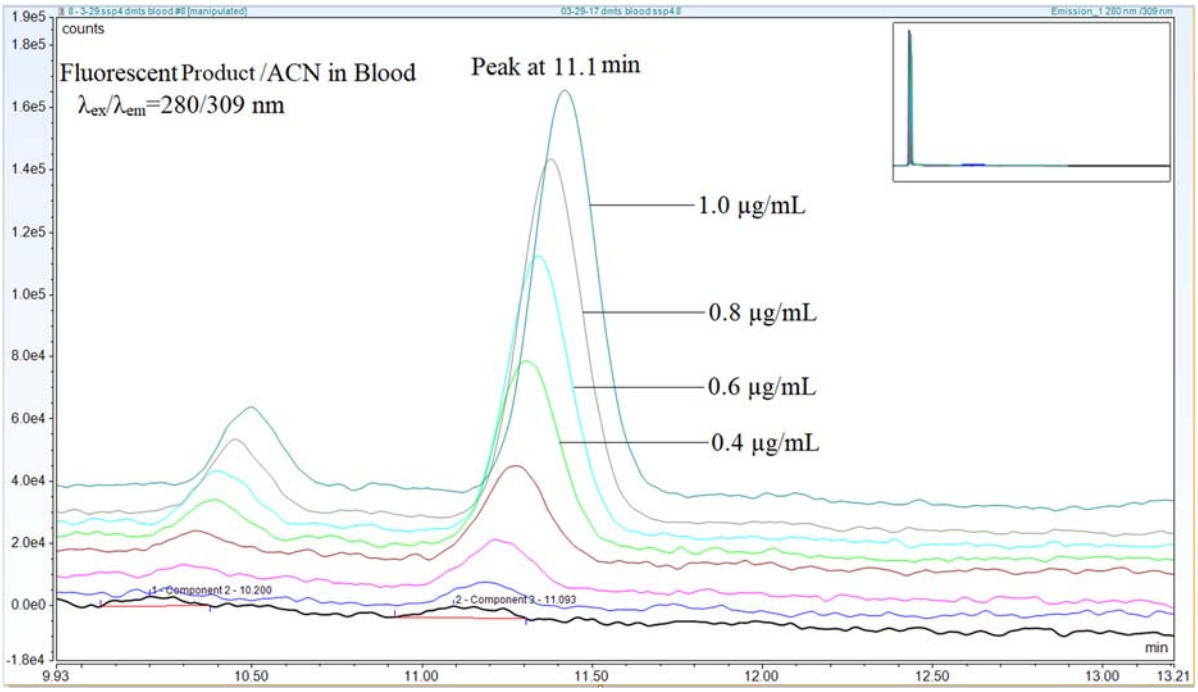

Figure 28. Proportionality of the Corresponding Peak for the Fluorescent Product at 11.1 min with DMTS/ACN Concentrations (0.025 – 1.0 µg/mL) in Blood.

Based on the chromatograms observed, the peak at 11.1 min was considered as the corresponding peak for the fluorescent product, yielded from the reaction between SSP4 and DMTS/ACN in blood. Since, the peak at 11.1 min showed a good proportionality with DMTS concentrations, it was used to quantify the concentration of DMTS/ACN in blood.

A calibration curve was developed by plotting the peak area at 11.1 min *vs*. DMTS concentrations in the range of 0.025 – 0.8 µg/mL.

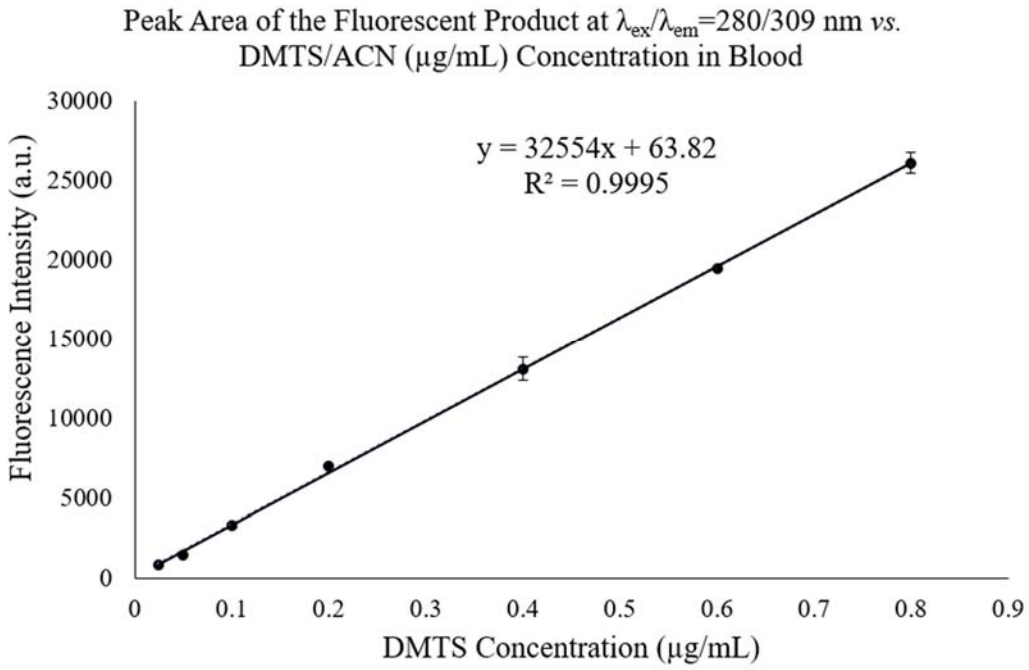

*Figure 29.*Calibration Curve for DMTS/ACN in Blood Measured using a Fluorescence Detector in HPLC. Data are presented as mean ± *s*; number of measurements (n) =3. Some error bars are not visible as the *s* is low.

DMTS concentrations between 0.025 µg/mL to 0.8 µg/mL gave good correlation with the fluorescence intensity. The resulting linear plot, shown in figure 29, had an R^2 value of 0.9995 and an equation of y = 32554x + 63.82.

The limit of detection (LOD) and limit of quantification (LOQ) were determined for the calibration curve.

$$LOD = y_{blank} + 3s = 138.17 + (3 \times 2.74) = 146.40$$

$$\text{Concentration LOD} = 3s/m = (3 \times 2.74)/32554 = 0.00025\ \mu g/mL$$

$$LOQ = y_{blank} + 10s = 138.17 + (10 \times 2.74) = 165.61$$

$$\text{Concentration LOQ} = 10s/m = (10 \times 2.74)/32554 = 0.00084\ \mu g/mL$$

Where y_{blank} is the mean of the blank signal, *s* is the standard deviation of the signal for the lowest analyzed concentration and *m* is the gradient of the calibration curve.

$s = \sqrt{\frac{(x_m - x_i)^2}{n-1}}$ where x_m is the mean of the repeats, x_i is the individual value of measurement and n is the number of repeats for the lowest analyzed concentration.

Accuracy (%) and precision (%) for the calibration curve are shown in table 10 and table 11.

Table 10

Accuracy (%) and Precision (%) for the Calibration Curve of Peak Area vs. DMTS/ACN Concentration (µg/mL) in Blood

Concentration of DMTS (µg/mL)	**Accuracy (%)**	**Precision (%)**
0.1	2.6870	0.8013
0.4	-1.3478	0.8633
0.8	-12.1642	0.4124

Table 11

Intraday and Interday Accuracy (%) for the Calibration Curve of Peak Area vs. DMTS/ACN Concentration (µg/mL) in Blood

Concentration of DMTS (µg/mL)	**Accuracy (%)**	
	Day 1	**Day 2**
0.1	-1.4189	-10.0967
0.2	6.4877	4.2202
0.4	0.1419	0.6679

CHAPTER IV

CONCLUSION

PART 1

Determination of *In Vitro* SD Efficacy of Three Different SDs using a Spectrophotometric SCN Assay at pH 7.4 and 8.6

SD_1 showed the highest SD_1 efficacy followed by SD_2 and SD_3. SD_1 showed the lowest Rh dependency at pH 7.4 and 8.6 while SD_2 and SD_3 showed higher Rh dependency at both pH values. Unlike SD_3, the SD_1 and SD_2 showed remarkable *in vitro* SD efficacies even at low doses.

Comparison of *In Vivo* Antidotal Efficacy of Three Different SDs in Mice

The antidotal efficacy of SD_1 was measured in our current experiments and was compared to that of SD_2 and SD_3. *In vivo* efficacy studies indicated that SD_2 has the highest antidotal efficacy (at the dose of 100 mg/kg the APR for SD_2 =3.2 while SD_1 and SD_3 provided only a very small antidotal protection, when administered IM (at the dose of 100 mg/kg the APR values for SD_1=1.4 and for SD_3=1.1).

For a good comparison, the dose of 100 mg/kg was selected for SD_1 because that dose was used earlier for SD_2 and SD_3.

The *in vitro* SD efficacy and *in vivo* antidotal efficacy comparison showed a different order for the antidotes tested. There can be numerous pharmacokinetic reasons for it, such as different bioavailability, membrane permeability and/or hydrophobicity.

PART 2

3D and 2D Scan of the Reaction Mixture Containing SSP4 and DMTS in ACN using Fluorescence Spectrophotometer

3D and 2D scans indicate that the reaction mixture of SSP4/water (50 μM, 300 μL) and DMTS/ACN (1 μg/mL, 3 mL) can be excited at 280 nm after which light is emitted at 309 nm wavelengths with a high fluorescence intensity. Therefore, it can be concluded that a formed fluorescent product from the reaction can be detected at $\lambda_{ex}/\lambda_{em}$=280/309 nm.

Calibration Curve to Determine Low Concentrations of DMTS in ACN using Fluorescence Spectrophotometer

Various DMTS/ACN concentrations in the range of 0 to 0.5 μg/mL showed good correlation with the fluorescence intensity of the fluorescent product formed. The resulting linear plot showed a good R^2 value of 0.9935 and an equation of y = 141213x – 1314.1. The signal of the fluorescent product in the reaction of SSP4/water (50 μM, 300 μL) and DMTS/ACN was proportional to the DMTS concentration up to 0.5 μg/mL. It was necessary to dilute the higher DMTS concentrations with ACN in order to get into the linear calibration range. Further studies will be run to obtain the intraday and interday data for the method validation.

Calibration Curve to Determine Low Concentrations of DMTS in ACN using Fluorescence Detector in HPLC

Selected excitation and emission wavelengths from the fluorescence spectrophotometric studies were used to analyze the fluorescent product of the reaction of DMTS/ACN with SSP4/water using a fluorescence detector in HPLC. The relevant peak of the fluorescent product was at 11.1 minutes at $\lambda_{ex}/\lambda_{em}$=280/309 nm on the

chromatogram. The area of this peak showed good correlation with the DMTS/ACN concentrations. The calibration curve for the peak area of the fluorescent product *vs*. DMTS concentrations in the range of 0.025 – 0.9 µg/mL µg/mL gave R^2 value of 0.9925 and an equation of y = 84919x – 2461.4. While the calibration curve for the peak area of the fluorescent product *vs*. DMTS concentrations in the range of 0.025 – 1.0 µg/mL µg/mL gave R^2 value of 0.993 and an equation of y = 87381x – 2987.4. Further studies will be run to obtain the interday data for the method validation.

Calibration Curve to Determine Low Concentrations of DMTS/ACN in Blood Samples using Fluorescence Detector in HPLC

The same HPLC- fluorescence detector method was used to obtain the calibration curve for DMTS/ACN in blood samples. The fluorescent product relevant peak was detected at 11.1 minutes at $\lambda_{ex}/\lambda_{em}$=280/309 nm on the chromatogram. This peak area of the fluorescent product was directly proportional to the DMTS/ACN concentrations. The calibration curve in the range of 0.025 – 0.8 µg/mL gave R^2 value of 0.9995 and an equation of y = 32554x – 63.82. Interday analysis data has shown a variation in the data. It can be due to many reasons including temperature variations between days. Therefore, it is required to adjust the temperature of the flow cell to the lowest possible in HPLC. To prevent the occurrence of those possible errors, a better solution would be to develop a calibration curve on the same day when the pharmacokinetic study is performed.

Future Recommendations

The structure of the fluorescent produced from the reaction of SSP4 and DMTS is remains to be determined in the future.

REFERENCES

(1) Coleby, L. J. M. A HISTORY OF PRUSSIAN BLUE. *Ann. Sci.* **1939**, *4*, 206–211.

(2) Macquer, P. J. Examen Chymique De Bleu de Prusse. *Mem. L' Acad. R. des. Sci. annee.* **1752**, 60–77.

(3) Crosland, M. *Gay-Lussac: SCIENTIST AND BOURGEOIS*; Cambridge University Press: London, 1978; pp 45-74.

(4) Huebnar, W. F.; Snyder, L. E.; Buhl, D. HCN radio emission from Comet Kohoutek (1973f). *Icarus.* **1974**, *23*, 580–584.

(5) Lieberei, R.; Biehl, B.; Giesemann, A.; Junqueira, N. T. V. Cyanogenesis Inhibits Active Defence Reactions in Plants. *Plant Physiol.* **1989**, *90*, 33–36.

(6) Petrikovics, I.; Budai, M.; Kovacs, K.; Thompson, D. E. Past, present and future of cyanide antagonism research: From the early remedies to the current therapies. *World J. Methodol.* **2015**, *5*, 88–100.

(7) Rockwood, G. A.; Thompson, D. E.; Petrikovics, I. Dimethyl trisulfide: A novel cyanide countermeasure. *Toxicol. lnd. Health.* **2016**, *32*, 2009–2016.

(8) Jensen, P.; Wilson, M. T.; Aasa, R.; Malmström, B. G. Cyanide inhibition of cytochrome c oxidase. A rapid-freeze e.p.r. investigation. *Biochem. J.* **1984**, *224*, 829–837.

(9) Okolie, N. P.; Osagie, A. U. Differential effects of chronic cyanide intoxication on heart, lung and pancreatic tissues. *Food Chem. Toxicol.* **2000**, *38*, 543–548.

(10) Ballantyne, B.; Bright, J.; Swanston, D. W.; Williams, P. Toxicity and Distribution of Free Cyanides given intramuscularly. *Med. Sci. Law.* **1972**, *12*, 209–219.

(11) Davies, B.; Morris, T. Physiological parameters in laboratory animals and humans.

Pharm. Res. **1993**, *10*, 1093–1095.

(12) Isom, G. E.; Borowitz, J. L.; Hall, A. H.; Rockwood, G. A. *Toxicology of Cyanide and Cyanogens:Experimental, Applied and Clinical Aspects*; Hall, A. H., Isom, G. E., Rockwood, G. A., Eds.; John Wiley and Sons, Ltd: West Sussex, 2015; pp 57-60.

(13) Way, J. L. CYANIDE INTOXICATION AND ITS MECHANISM OF ANTAGONISN. *Ann. Rev. Pharmacol. Toxicol.* **1984**, *24*, 451–481.

(14) Westley, J. Thiosulfate: Cyanide sulfurtransferase (rhodanese). *Methods Enzymol.* **1981**, *77*, 285–291.

(15) Dixon, W. J.; Massey, F. J. *INTRODUCTION TO STATISTICAL ANALYSIS*; 4th ed.; McGraw-Hill: New York, 1983; pp 426-441.

(16) Moore, S. J.; Norris, J. C.; Walsh, D. A.; Hume, A. S. Antidotal use of methemoglobin forming cyanide antagonists in concurrent carbon monoxide/cyanide intoxication. *J. Pharmacol. Exp. Ther.* **1987**, *242*, 70–73.

(17) Christel, D.; Eyer, P.; Hegemann, M.; Kiese, M.; Lorcher, W.; Weger, N. Pharmacokinetics of cyanide in poisoning of dogs, and the effect of 4-dimethylaminophenol or thiosulfate. *Arch. Toxicol.* **1997**, *38*, 177–189.

(18) Way, J. L. Cyanide Antagonism. *Fundam. Appl. Toxicol.* **1983**, *3*, 383–386.

(19) Norris, J. C.; Utley, W. A.; Hume, A. S. Mechanism of antagonizing cyanide-induced lethality by alpha-ketoglutaric acid. *Toxicology.* **1990**, *62*, 275–283.

(20) Isom, G. E.; Johnson, J. D. *Sulfur donors in cyanide intoxication. In Clinical and Experimental Toxicology of Cyanides*; Ballantyne, B., Marrs, T. C., Eds.; Wright Pub: Bristol, 1987; pp 413-426.

(21) Voegtlin, C.; Johnson, J. M.; Dyer, H. A. Biological significance of cystine and glutathione on the mechanism of the cyanide action. *J. Pharmacol. Exp. Ther.* **1926**, *27*, 467–483.

(22) Marraffa, J. M.; Cohen, V.; Howland, M. A. Antidotes for toxicological emergencies: A practical review. *Am. J. Heal. Pharm.* **2012**, *69*, 199–212.

(23) Petrikovics, I.; Baskin, S. I.; Beigel, K. M.; Schapiro, B. J.; Rockwood, G. A.; Manage, A. B.; Budai, M.; Szilasi, M. Nano-intercalated rhodonese in cyanide antagonism. *Nanotoxicology.* **2010**, *4*, 247–254.

(24) Chen, K. K.; Rose, C. Nitrite and thiosulfate therapy in cyanide poisoning. *J. Am. Med. Assoc.* **1952**, *149*, 113–119.

(25) Kovacs, K.; Jayanna, P. K.; Duke, A.; Winner, B.; Negrito, M.; Angalakurthi, S.; Yu, J. C. C.; Furedi, P.; Ludanyi, K.; Sipos, P.; Rockwood, G. A.; Petrikovics, I. A Lipid Base Formulation for Intramuscular Administration of a Novel Sulfur Donor for Cyanide Antagonism. *Curr. Drug Deliv.* **2016**, *13*, 1351–1357.

(26) Petrikovics, I.; Cannon, E. P.; McGuinn, W. D.; Pei, L.; Way, J. L. Cyanide Antagonism with Organic Thiosulfonates and Carrier Red Blood Cells Containing Rhodanese. *Fundam. Appl. Toxicol.* **1995**, *24*, 1–8.

(27) Block, E. The Chemistry of Garlic and Onions. *Sci. Am.* **1985**, *252*, 94–99.

(28) Ayala-Zavala, J. F.; González-Aguilar, G. A.; Del-Toro-Sánchez, L. Enhancing safety and aroma appealing of fresh-cut fruits and vegetables using the antimicrobial and aromatic power of essential oils. *J. Food Sci.* **2009**, *74*, 84-91.

(29) Way, J.; Sylvester, D.; Morgan, R.; Isom, G.; Burrows, G.; Tamulinas, C. Recent Perspectives on the Toxicodynamic Basis of Cyanide Antagonism. *Fundam. Appl.*

Toxicol. **1984**, *4*, 231-239.

(30) Petrikovics, I.; Baskin, S. I.; Rockwood, G. A. Dimethyl Trisulfide as a Cyanide Antidote. US20150290143 A1, 2015.

(31) Petrikovics, I.; Kovacs, K. Formulations of Dimethyl Trisulfide for Use as a Cyanide Antidote. US9456996 B2, 2015.

(32) Toohey, J. I. Sulphane sulphur in biological systems: a possible regulatory role. *Biochem. J.* **1989**, *264*, 625–632.

(33) Hol, W. G. L.; Lijk, L. J.; Kalk, K. H. The High Resolution Three-Dimensional Structure of Bovine Liver Rhodanese. *Fundam.Appl.Toxicol.* **1983**, *3*, 370–376.

(34) Spallarossa, A.; Forlani, F.; Carpen, A.; Armirotti, A.; Pagani, S.; Bolognesi, M.; Bordo, D. The "rhodanese" fold and catalytic mechanism of 3-mercaptopyruvate sulfurtransferases: crystal structure of SseA from Escherichia coli. *Mol.Biol.* **2004**, *335* : 583–593.

(35) Cianci, M.; Gliubich, F.; Zanotti, G.; Berni, R. Specific interaction of lipoate at the active site of rhodanese1. *Biochim. Biophys. Acta - Protein Struct. Mol. Enzymol.* **2000**, *1481*, 103–108.

(36) Westley, J. Rhodanese. *Adv Enzym. Areas Mol. Bio.l* **1973**, *39*, 327–368.

(37) Cerletti, P. Seeking a better job for an underemployed enzyme : rhodanese. *Trends Biochem. Sci.* **1986**, *11*, 369–372.

(38) Ogata, K.; Volini, M. Mitochondrial Rhodanese:membrane Bound and Complex Activity. *J. Biol. Chem.* **1990**, *265*, 8087–8093.

(39) Nandi, D. L.; Horowitz, P. M.; Westley, J. Rhodanese as a thioredoxin oxidase. *Int. J. Biochem. Cell Biol.* **2000**, *32*, 465–473.

(40) Isom, G. E.; Borowitz, J. L.; Mukhopadhyay, S. *Sulfurtransferases Enzymes Involved in Cyanide Metabolism*; 3rd ed.; McQueen, C. A., Eaton, D. L., Eds.; Elsevier Ltd.: Amsterdam, 2010; pp 485-498.

(41) Marrs, T. C. *The Choice of Cyanide Antidotes. In Clinical and Experimental Toxicology of Cyanides*; Ballantyne, B., Marrs, T. C., Eds.; Wright Pub: Bristol, 1987; pp 312-333.

(42) Alexander, K.; Volini, M. Properties of an Escherichia coli Rhodanese. *J. Biol. Chem.* **1987**, *262*, 6595–6604.

(43) Valeur, B.; Berberan-Santos, M. N. A Brief History of Fluorescence and Phophorescence Before the Emergence of Quantum Theory. *J. Chem. Educ.* **2011**, *88*, 731–738.

(44) Braslavsky, S. E. GLOSSARY OF TERMS USED IN PHOTOCHEMISTRY, *Pure Appl. Chem.* **2007**, *79*, 293–465.

(45) Stokes, G. G. On the Change of Refrangibility of Light. *Phil. Trans. R. Soc. Lond.* **1852**, *142*, 463–562.

(46) Lakowicz, J. R. *Principles of Fluorescence Spectroscopy*; 3rd ed.; Springer: New York, 2006; pp 1-15.

(47) Arrowsmith, C. H.; Audia, J. E.; Austin, C.; Baell, J.; Bennett, J.; Blagg, J.; Bountra, C.; Brennan, P. E.; Brown, P. J.; Bunnage, M. E.; Carolyn Buser-Doepner, R. M. C.; Carter, A. J.; Cohen, P.; Copeland, R. A.; Cravatt, B.; Dahlin, J. L.; Dhanak, D.; Edwards, A. M.; Frederiksen, M.; Frye, S. V.; Gray, N.; Grimshaw, C. E.; Hepworth, D.; Howe, T.; Huber, K. V. M.; Jin, J.; Knapp, S.; Kotz, J. D.; Kruger, R. G.; Lowe, D.; Mader, M. M.; Marsden, B.; Mueller-Fahrnow, A.; Müller, S.; O'Hagan, R. C.;

Overington, J. P.; Owen, D. R.; Rosenberg, S. H.; Ross, R.; Roth, B.; Schapira, M.; Schreiber, S. L.; Shoichet, B.; Sundström, M.; Superti-Furga, G.; Taunton, J.; Toledo-Sherman, L.; Walpole, C.; Walters, M. A.; Willson, T. M.; Workman, P.; Young, R. N.; Zuercher, W. J. The promise and peril of chemical probes. *Nat. Chem. Biol.* **2015**, *11*, 536–541.

(48) http://www.dojindo.com/store/p/952-SulfoBiotics-SSP4.html (accessed Oct 24, 2017)

(49) Harris, D. C. *Quantitative Chemical Analysis*; 8th ed.; W.H Freeman and Company: New York, 2010; pp 102.

APPENDIX

Glossary

CN: cyanide

CN^-: cyanide anion

Rhodanese: Rh

SD: sulfur donor

SD_1: sulfur donor 1

SD_2: sulfur donor 2

SD_3: sulfur donor 3

SSP4: sulfane sulfur probe

DMTS: dimethyl trisulfide

SwRI: Southwest Research Institute

poly 80: polyoxyethylenesorbitan monooleate

span 80: sorbitan monoenolate

HPLC: high pressure liquid chromatography

IM: intramuscular

s: sample standard deviation

VITA

Ramesha Dilhani Gaspe Ralalage

Education

2016-present M.S. in chemistry, Sam Houston State University, Huntsville, TX, US

2008–2013 B.Sc. in chemistry, University of Kelaniya, Dalugama, Sri Lanka

Academic Employment

2016-present Teaching Assistant, Chemistry Department, Sam Houston State University

- Instructed students in the following course labs: Inorganic and Environmental Chemistry, General Chemistry II, Introductory Organic and Biochemistry, Organic Chemistry I.
- Specific work included lab set up and maintenance, evaluation of examinations, assignments, and lab reports. 20 hours per week, each semester.

Publications

Gaspe Ralalage, R.D., Hewa Rahinduwage, C.C., Warnakula, I.K., Rios, C.T.S., Kiss, M., Roy, R.J., Baca, W., Ebrahimpour, A., Petrikovics, I. Comparison of three different cyanide antidote candidate sulfur donor molecules *in vitro* and *in vivo.* ACS Regional meeting, October 29 November 01, **2017**, Lubbock, TX. (Abstract No: 2821922, Poster No: 296).

Rios, C.T.S., Vergara, M.N., Ebrahimpour, A., Kiss, M., Warnakula, I.K., **Gaspe Ralalage, R.D.**, Hewa Rahinduwage, C.C., Barrera, I., Petrikovics, I. *In vitro* and *in vivo* characterization of the cyanide antidote SDX6F2. ACS Regional meeting, October 29 - November 01, **2017**, Lubbock, TX. (Abstract No: 2821909, Poster No: 62).

Warnakula, I.K., Kiss, M., Rios, C.T.S., Vergara, M.N., **Gaspe Ralalage, R.D.**, Barcza, T., Petrikovics, I. Redox reactions with dialkyl polysulfides. ACS Regional meeting, October 29 November 01, **2017**, Lubbock, TX. (Abstract No: 2821927, Poster No: P335).

Gaspe Ralalage, R. D.; Hewa R, C. C.; Veltman, K.; Logue, B.; Thompson, D.; Petrikovics, I.; Ebrahimpour, A. Fluorescent detection method for the cyanide antidote SDX6 using a sulfane sulfur probe. 55th SOT Annual Meeting, March 12-16, **2017**, Baltimore, MD. (Abstract No: 2073, Poster No: P235).

Hewa R., C. C.; **Gaspe Ralalage, R. D.**; Warnakula, I.K; Preethika D. K. N.; Kiss, L.; Ebrahimpour, A.; Petrikovics, I.; Characterization of the cyanide antidote candidate SAX6 in two formulation forms: Blood Brain Barrier(BBB) penetration, Size

distribution, *In vivo* efficacy and Pharmacokinetics. 55th SOT Annual Meeting, March 12-16, **2017,** Baltimore, MD. (Abstract No: 2052, Poster No. P214).

Gaspe Ralalage, R.D., Hewa R., C.C., Ebrahimpour, A., Petrikovics, I., *In vitro* sulfur donor reactivity of various cyanide antidote candidates. Texas Academy of Science, Annual Meeting, March **2017**, Belton, Texas. (Oral Presentation No: 007.006 G).

Gaspe Ralalage, R. D.; Hewa R, C. C.; Ebrahimpour, A.; Petrikovics, I. Different Sulfur Donor Efficacy for Cyanide Intoxication in vitro. ACS SWRM meeting, November 10-13, **2016**, Galveston, Texas. (Abstract and Poster No: 498).

Kiss, L., Ebrahimpour, A.; Hewa R., C. C.; **Gaspe Ralalage, R.D.**; Dong, X.; Deli, M.; Sipos, P.; Revesz, P.; Thompson, D.E.; Rockwood, G.A.; Petrikovics, I. Antidotal Efficacy and Pharmacokinetics of Dimethyl Trisulfide (DMTS) as a Novel Cyanide (CN) Antidote. 20th Biannual Medical Defense Bioscience Review. **2016**, June 6-9, US Army Medical Research Institute of Chemical Defense, Aberdeen Proving Ground, MD. (Poster No: 071)

Hewa R., C. C.; **Gaspe Ralalage, R. D.**; Ebrahimpour, A.; Petrikovics, I. Determining the Surfactant and Stirring Effects on the Permeability of Dimethyl Trisulfide (DMTS) in the Parallel Artificial Membrane Permeability Assay (PAMPA). ACS SWRM meeting, November 10-13, **2016**, Galveston, Texas. (Abstract and Poster No: 544)

Hewa R, C. C.; **Gaspe Ralalage, R. D.**; Warnakula, I.K.; Ebrahimpour, Afshin; Petrikovics, I. Modelling Blood Brain Barrier (BBB) penetration by *in vitro* permeability study with the newly formulated cyanide (CN) antidote, dimethyl trisulfide (DMTS), Texas Academy of Science Annual Meeting, March **2017**, Belton, Texas. (Oral presentation No: 017.044 G).

Carpenter, M., Kefer, E., Veltman, K., **Gaspe Ralalage, R.D.**, Ebrahimpour, A., Petrikovics, I.Blood Partitioning of SDMEK, a New Cyanide Antidote, ACS SWRM meeting, November 10-13, **2016**, Galveston, Texas.

Weeraratne, K.S., Buwaneka, P.A., **Gaspe Ralalage, R. D.**; Jayathilaka, N (2014). Epigenetic modifications in human disease. Kalyani Journal of the University of Kelaniya, 30(**2015**) 79.

Gaspe Ralalage, R. D.; Jayalath, K.G., Deeyamulla, M. P., Assessment of atmospheric metal pollution in Bat-taramulla using high volume air sampler and *Hyophila involuta* biomonitor, Proc. Sri Lanka Ass. Adv. Sci., 70 (**2014**) 81.

Awards and Honors

- Sam Houston State University (SHSU) Chemistry Academic Scholarship - Summer 2016
- Robert Welch Foundation - Academic Year 2015-2016 and 2016-2017
- SHSU Graduate Studies Scholarships - Academic Year 2015-2016 and 2016-2017
- Special- COAS Scholarships - Academic Year 2017-2018